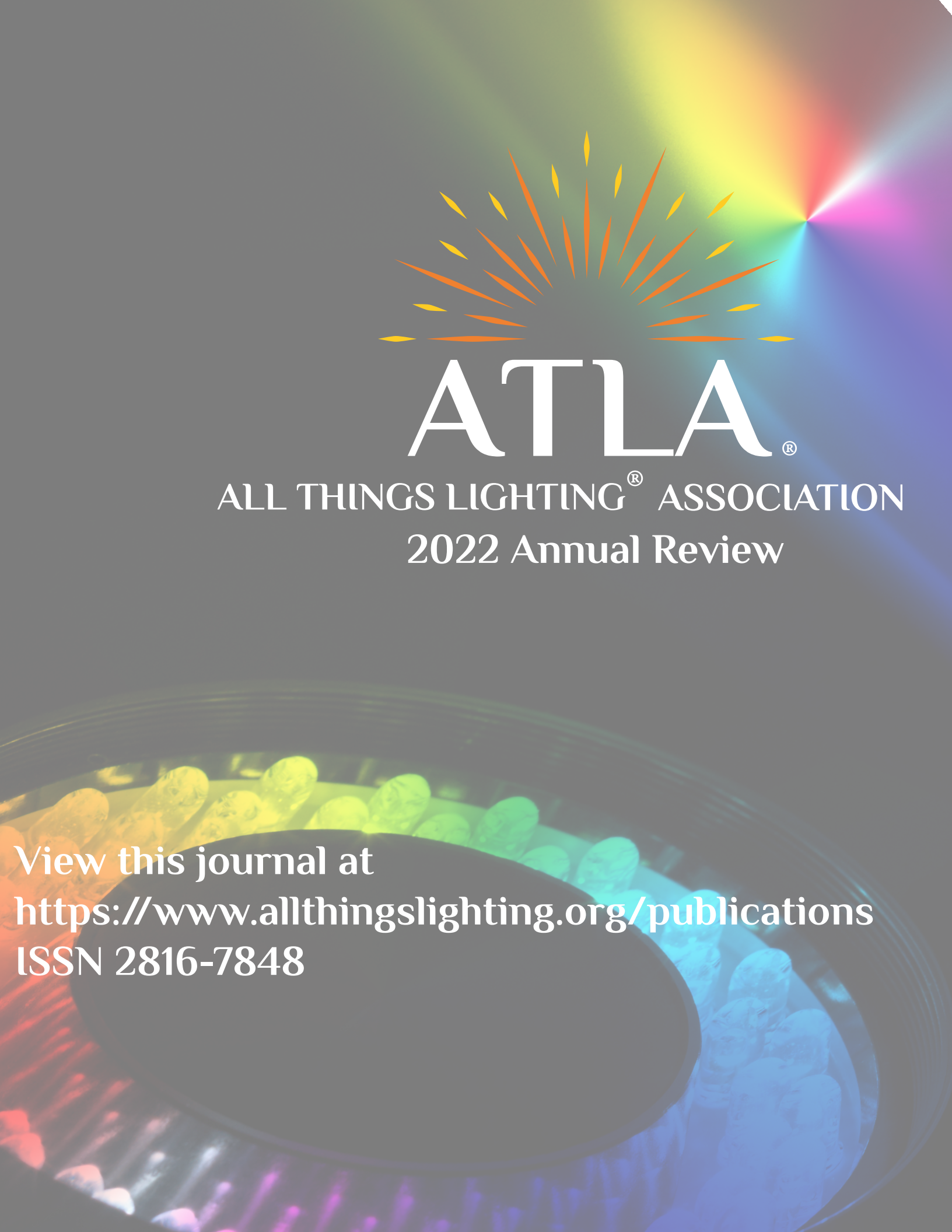

View this journal at
https://www.allthingslighting.org/publications
ISSN 2816-7848

ALL THINGS LIGHTING® ASSOCIATION

Contributor- Ian Ashdown, Senior Scientist

CONTENTS

ALL THINGS LIGHTING

View this journal at https://www.allthingslighting.org/publications

HORTICULTURAL INFORMATION

LIGHTING UNIFORMITY IN HORTICULTURE

Ian Ashdown, P. Eng., FIES, Senior Scientist, SunTracker Technologies Ltd. Published: 22/06/23

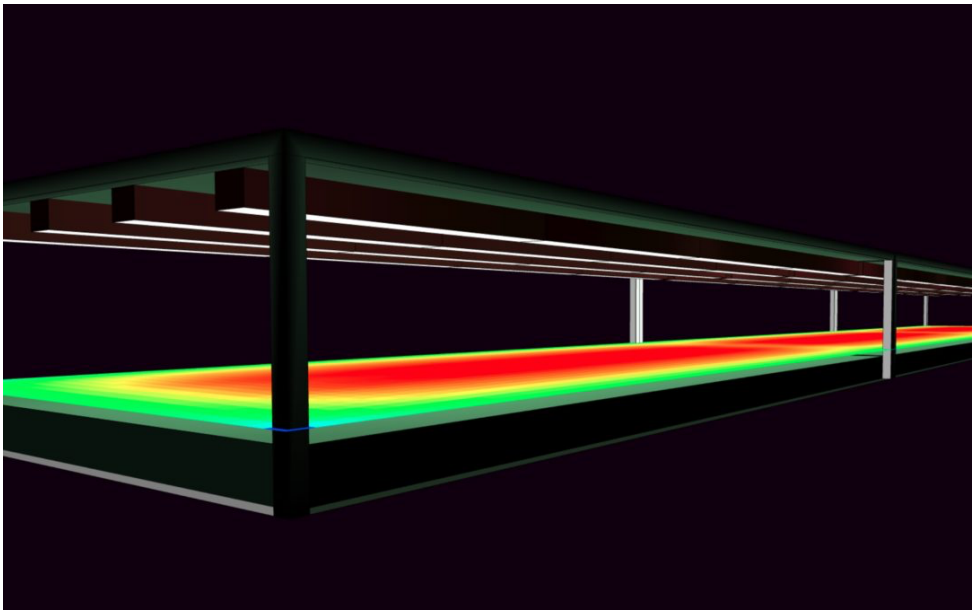

AUTHORS: IAN ASHDOWN, SENIOR SCIENTIST AND MARC DESCOTEAUX, SENIOR SOFTWARE ENGINEER, SUNTRACKER TECHNOLOGIES LTD.

Written in 2015, "Greenhouse Design and Control" (Ponce et al. 2015) is extraordinarily comprehensive in its coverage of greenhouse design issues, from site selection through structural load bearing analysis and ventilation technologies to greenhouse automation using adaptive neural fuzzy inference systems. On the topic of greenhouse lighting, however, it has only this to say:

"The light level in the greenhouse should be adequate and uniform for crop growth."

The authors note that quantum (PAR) sensors are commonly used for photosynthetic photon flux density (PPFD) measurements, but give no guidance on how to measure the lighting uniformity in a greenhouse. This topic has been occasionally discussed in the literature (Both et al. 2002, Ciolkosz et al. 2001, Eaton 2021, Ferentinos et al. 2005, Runkle 2017), but only in the context of supplemental lighting using lighting design software intended for architectural applications. The combination of ever-changing daylight and electric lighting has yet to be considered.

None of these discussions however address the central question:

what is "lighting uniformity" in horticulture, and how do we measure (or predict) it?

ARCHITECTURAL LIGHTING

Lighting uniformity in architecture has been a topic of interest for at least seventy years (e.g., IES 1947), where the goal is to encompass the range of illuminance values measured at an array of positions on a horizontal plane, all in a single metric. These metrics include:

- Coefficient of Variation (Armstrong 1990)
- Entropy-based (Mahdavi and Pal 1999)
- Maximum to average
- Maximum to minimum
- Minimum to average (EN 12464-1)
- Minimum to maximum
- Statistical (Mathieu 1989)
- Uniformity Gradient (Houser et al. 2011)

In practice, only the minimum-to-average illuminance metric is recognized as an international standard (EN 12464-1) for interior lighting design. This is sometimes designated as "U1," while the minimum-to-maximum illuminance metric is designated as "U2."

To be honest however, uniformity metrics represent a very simplistic approach to architectural lighting design. They make sense when illuminating large flat surfaces outdoors, such as sports fields, parking lots, and roadway interchanges, but for most interior lighting design applications, they provide little useful information.

HORTICULTURAL LIGHTING

Both the U1 and U2 metrics have been proposed for use in horticultural lighting design by a few luminaire manufacturers, where photosynthetic photon flux density (PPFD, measured in $\mu mol/m^2\text{-}s$) replaces illuminance (lux). This again makes sense because with overhead lighting and daylight, the plant canopy can usually be considered as a large flat surface.

The problem however is that while we perceive visible light reflected from surfaces, plants utilize it for their photosynthetic needs. What we might consider to be almost imperceptible differences in illuminance may be significant in terms of photosynthetic activity and hence plant growth and yield.

Commercial growers have for many decades relied on a rule of thumb that a one percent increase in sustained PPFD (and hence Daily Light Integral) results in a one percent increase in plant growth and yield. Marcelis et al. (2006) quantified this assumption by analyzing yield data from some one hundred academic papers and nearly ninety commercial growers, followed by opinion surveys with eighteen growers. Their research results are summarized in Table 1.

Crop Group	Crop	Yield Difference
Soil-grown vegetables	Lettuce	0.8%
	Radish	1.0%
Fruit vegetables	Cucumber	0.7 – 1.0%
	Tomato	0.7 – 1.0%
	Sweet pepper	0.8 – 1.0%
Cut flowers	Rose	0.8 – 1.0%
	Chrysanthemum	0.6%
Bulb flowers	Freesia	0.25 – 1.25%
	Lily	0.25 – 1.25%
Flowering pot plants	Poinsettia	0.5 – 0.7%
	Kalanchoe	0.8 – 1.0%
Non-flowering pot plants	Ficus	0.65%
	Dracaena	0.65%

Table 1 – Crop yield difference for one percent difference in sustained PPFD. Source: Marcelis et al. (2006).

The study results are of course more nuanced than this. For example, the yield difference is greater at lower PPFD levels, higher CO_2 concentrations, higher ambient temperatures, and leaf area index. As a result, growers may choose higher temperatures and change their plant density and cultivar choice during times of greater DLI or increased supplemental light levels. In other words, light levels are only one component of farm management.

The key point here however is that uniformity matters when it comes to horticultural lighting. For example, the two gray squares shown in Figure 1 may appear to be almost the same shade of gray to us, but for many plants, they represent a ten percent or so difference in photosynthetic activity and hence plant yield.

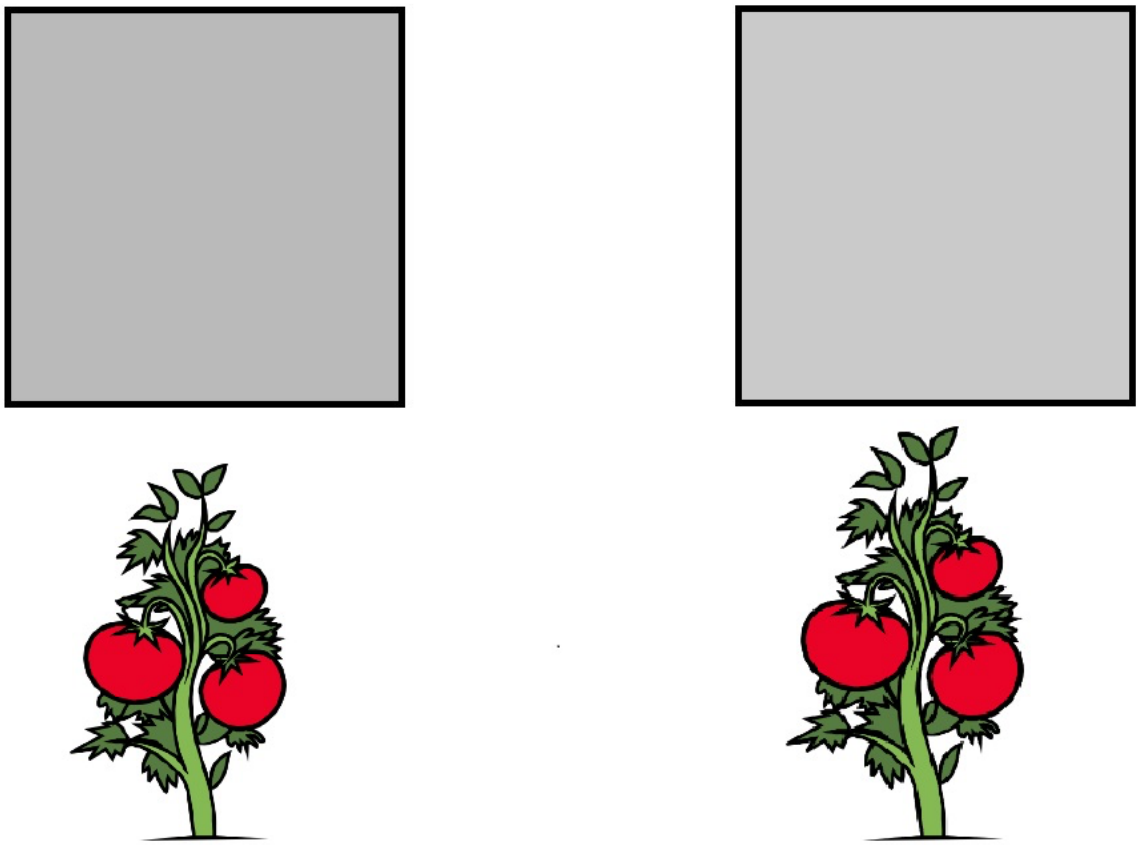

Figure 1 – What we see versus what plants respond to.

Given this, Runkle (2017) has recommended that, “Generally, a 10-20 percent variation in intensity is acceptable.” However, Yelton (2017) and others have proposed that ±5 percent is a more appropriate target for PPFD measurements in greenhouses and plant factories. Figure 1 shows a ten percent difference in plant yield in response to a ten percent increase in PPFD.

HORTICULTURAL UNIFORMITY METRIC

This suggests yet another uniformity metric, but one that is designed specifically for horticultural lighting. Suppose we are given a virtual model of a small 64×128-foot greenhouse with PPFD values due to electric lighting calculated at two-foot intervals (Figure 2). There are 2048 values, with a maximum of 291.3 µmol/m^2-s. The proposed lighting uniformity metric U_{90} is defined as the percentage of values that are greater than 90 percent of the maximum value, while the proposed lighting uniformity metric U_{80} is similarly defined as the percentage of values that are greater than 80 percent of the maximum value. (The measurement positions are assumed to be regularly spaced.)

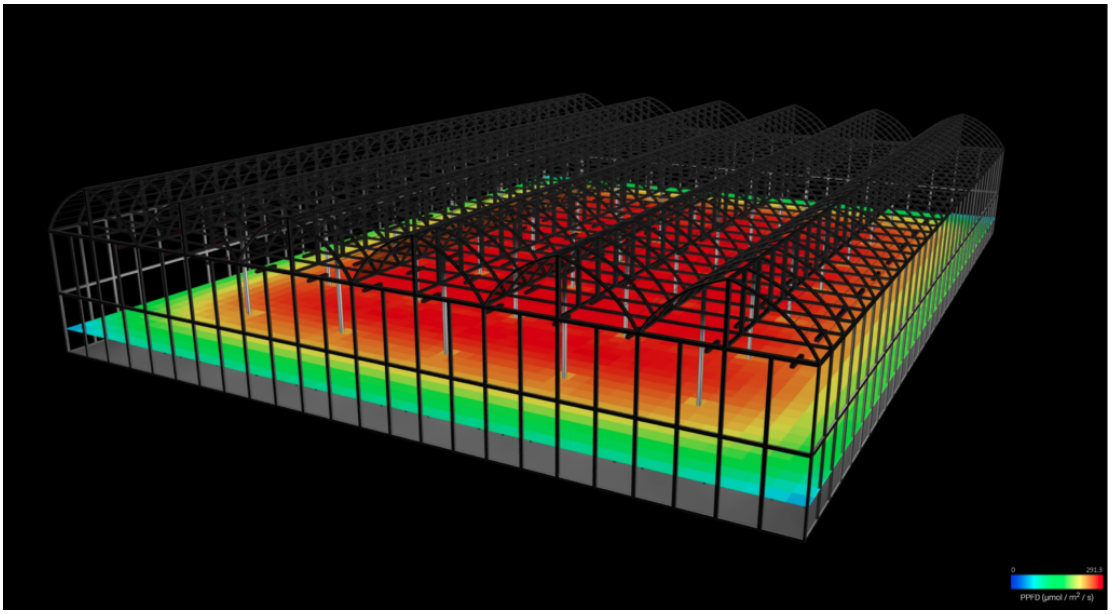

Figure 2 – PPFD distribution in a 64×128-foot greenhouse.

Unlike the architectural U1 and U2 metrics, these two metrics are particularly useful in that they indicate the relative floor area of the greenhouse that is suitable for growing crops. The U_{90} metric indicates the percentage of illuminated area that satisfies the ±5 percent uniformity requirement, while the U_{80} metric indicates the percentage of illuminated area that satisfies the ±10 percent uniformity requirement.

Even more useful is that these metrics can be shown in an isoPPFD plot (Figure 3).

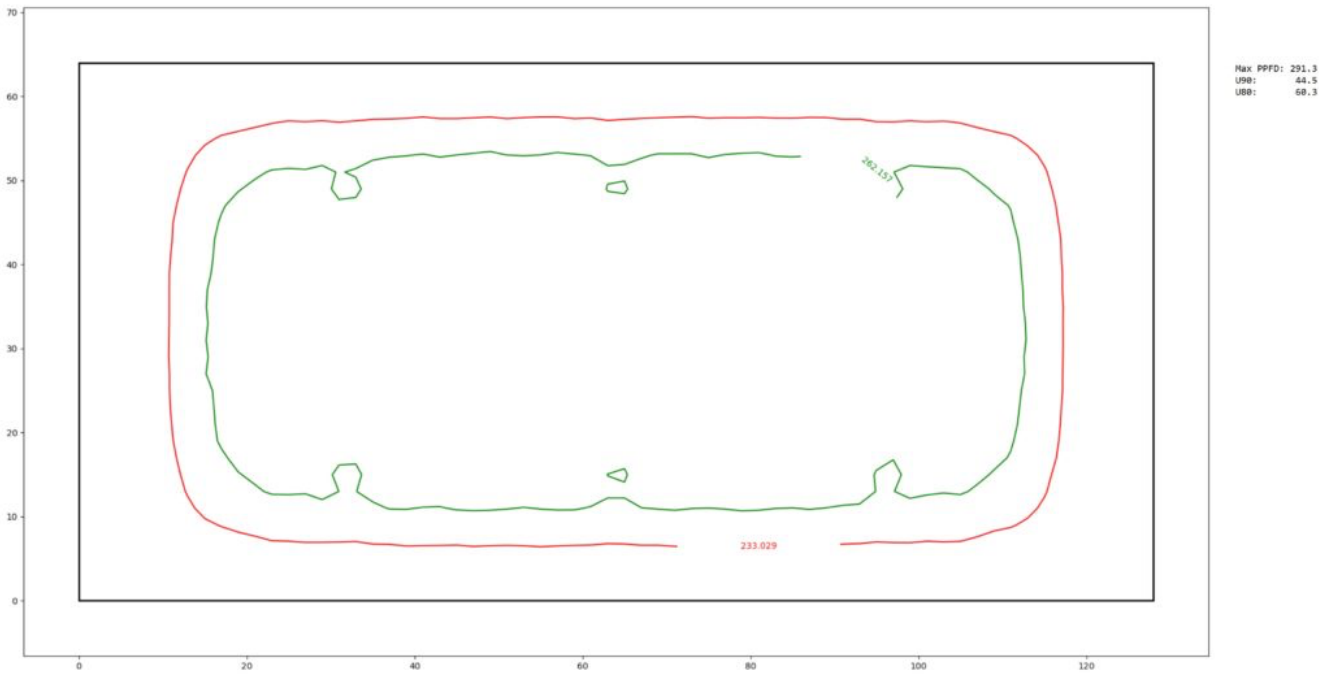

Figure 3 – Small greenhouse isoPPFD plot.

The first reaction will of course be that 44.5 percent usable floor area is terrible in terms of lighting uniformity. This however is precisely the point – the lighting uniformity in a small greenhouse with a regular array of identical luminaires will always be terrible. However, the nonuniformity is due to the area adjacent to the greenhouse walls. Yelton et al. (2017) noted that the uniformity can often be improved by varying the mounting height of the luminaires adjacent to the greenhouse walls, but this may not be an option for practical reasons.

Figure 4 shows a rendering of a commercial greenhouse measuring 512×1024 feet, with 7,680 luminaires, while Figure 5 shows its isoPPFD plot. The U_{90} metric is 90.0 percent, with the non-uniform areas confined to the floor area adjacent to the greenhouse walls.

Figure 4 – 512×1024-foot commercial greenhouse.

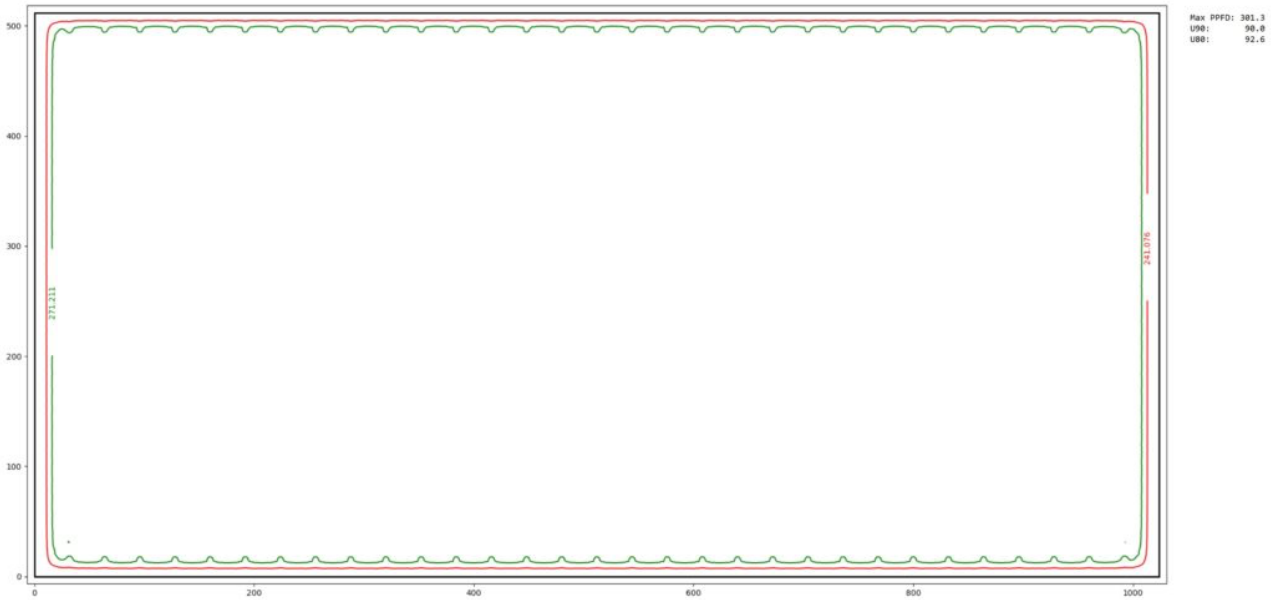

Figure 5 – Commercial greenhouse isoPPFD plot.

The U_{90} uniformity metric is excellent, but it should be noted that the lighting layout for the commercial greenhouse was chosen to ensure uniformity. Without lighting calculations to validate the uniformity, it cannot be assumed that a given design will satisfy the U_{90} requirements.

DAYLIGHT

We must also remember that the Daily Light Integral (DLI) inside greenhouses is due mainly to daylight, which is much more uniform. Figure 6, for example, shows the monthly average DLI for July with the same greenhouse located in Vancouver, Canada, based on Typical Meteorological Year (TMY3) weather records and solar radiation data from the EUMETSAT weather satellite (Thomas and Ashdown 2022).

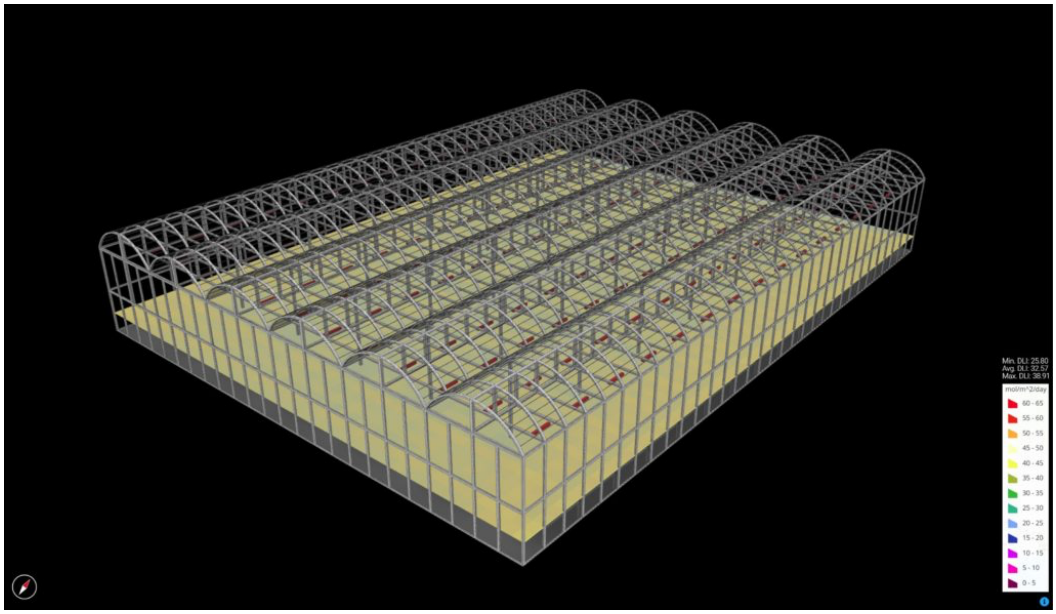

Figure 6 – Monthly average DLI distribution (Vancouver, Canada. July 1970).

VERTICAL FARMS

Where the U_{80} and U_{90} metrics become more interesting is in fully-enclosed plant factories, particularly stacked trays in vertical farms. Electrical energy represents between 25 and 35 percent of vertical farm operating costs, and so lighting uniformity for trays is a significant issue.
Figure 7 shows three trays measuring 2.1 feet wide by 4.9 feet long, and with a height of 11 inches. The plant canopy height is 1.8 inches. The four rows of luminaires are spaced at 8.0-inch intervals, which appear to provide good uniformity.

Three trays are modeled because, as we saw at the borders of the greenhouse models, we can expect there to be light drop-off at the tray ends.

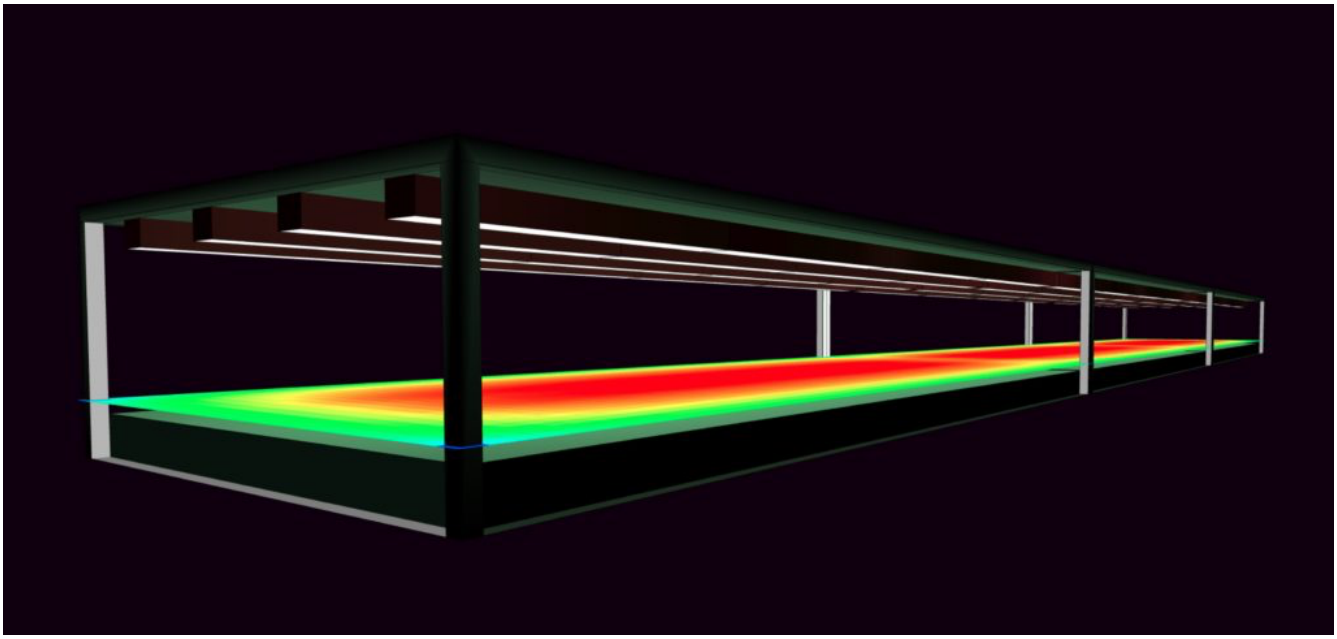

Figure 7 – Vertical farm tray PPFD distribution – canopy height 1.8 inches.

The isoPPFD plot shown in Figure 8, however, shows rather poor uniformity – only 40 percent of the canopy is within the desired ±5 percent uniformity for consistent crop yield.

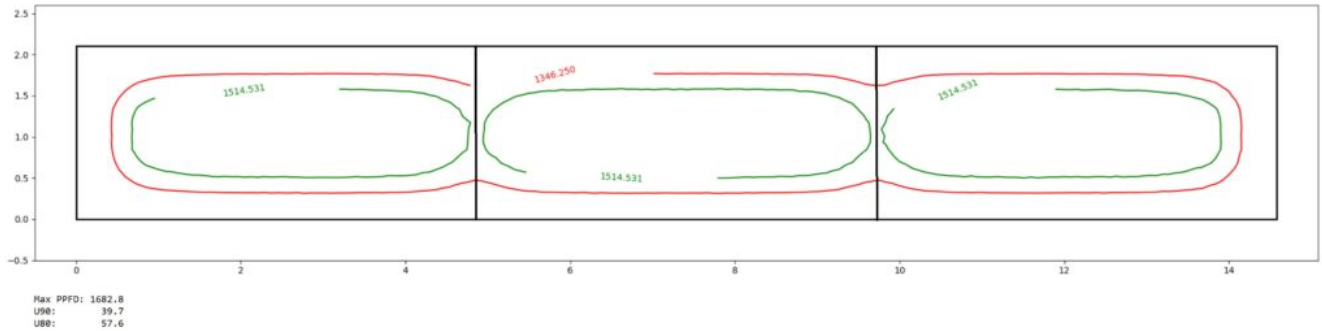

Figure 8 – Vertical farm trays isoPPFD plot – canopy height 1.8 inches.

Equally important is that these results are for plants in the seedling stage. As they mature, the canopy height increases to perhaps four inches or so. As they do, the lighting uniformity will decrease. Figure 9 shows the PPFD distribution for a plant height of 4.2 inches, where the uniformity is obviously less.

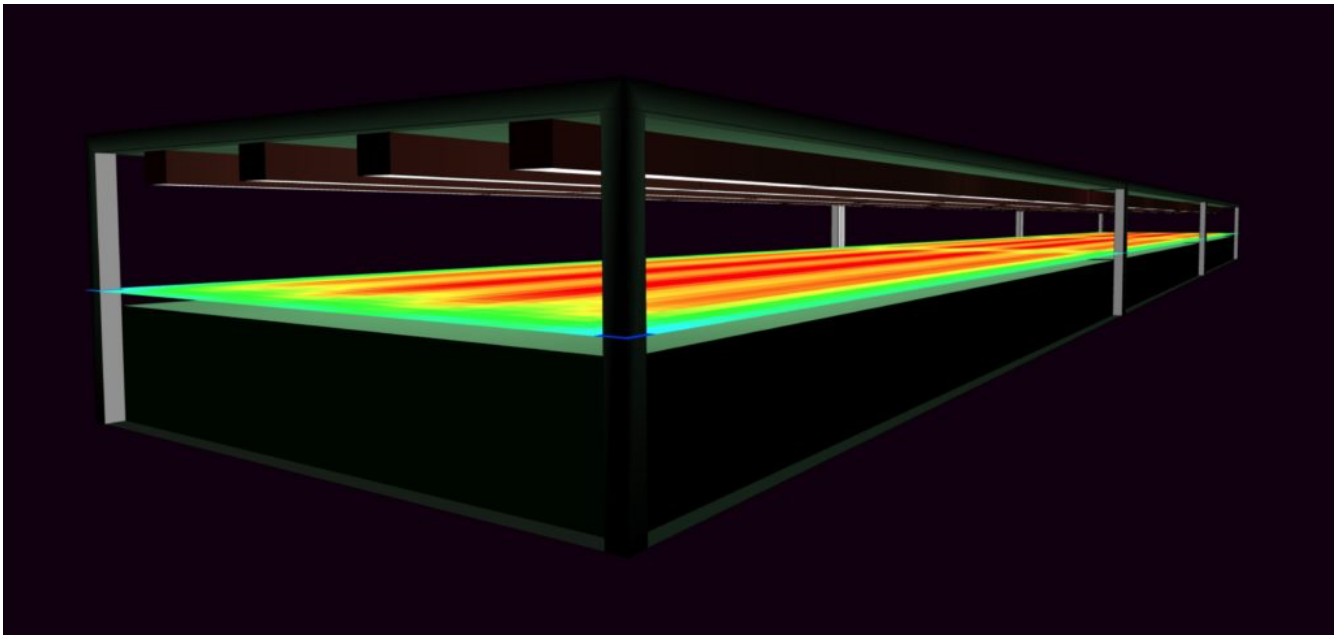

Figure 9 – Vertical farm tray PPFD distribution – canopy height 4.2 inches.

Figure 10 confirms this observation, where the U_{90} metric is only 21 percent.

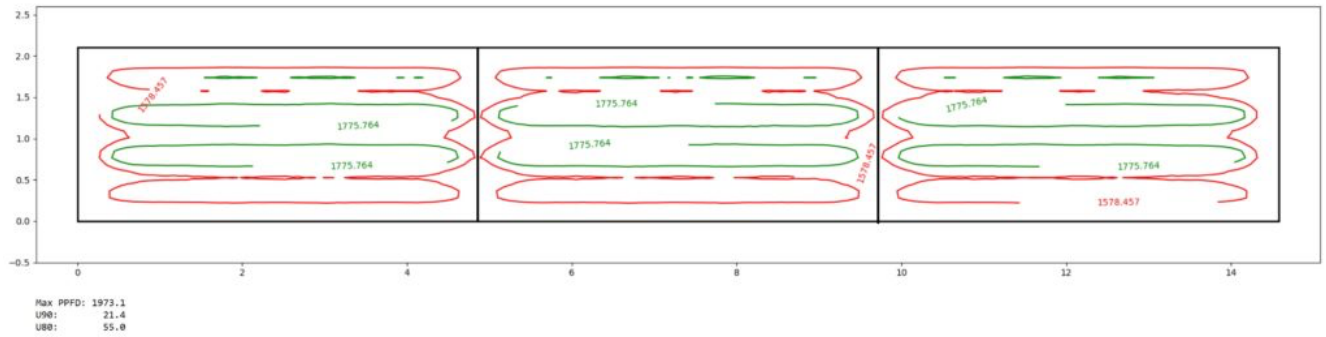

Figure 10 – Vertical farm trays isoPPFD plot – plant height 4.2 inches.

To be fair, the tray height of 11 inches is unusually low. It was chosen specifically to highlight the importance of taking the change in canopy height into consideration when designing tray lighting systems. Greater tray heights will result in improved uniformity, but then reducing the number of luminaire rows for example from four to three will significantly reduce the consistent growing area.

Speaking of tray lighting, there is another issue that uniformity metrics cannot address – spill light. Most horticultural luminaires designed for tray lighting do not include optics to control the beam spread, and so there will be a significant amount of light that ends up on the aisle floor rather than the plant canopy. Properly designed luminaire optics could address this issue to both save electrical energy (and money) and improve lighting uniformity.

SUMMARY

Simply viewing an installed lighting system for a greenhouse or vertical farm will not indicate whether the lighting uniformity is acceptable, and measuring it by hand is a time-consuming and laborious process that may be complicated by the existing infrastructure. It is much better if the uniformity can be calculated during the design stage.

To this end, the U_{90} and U_{80} lighting uniformity metrics presented here are specific to horticultural rather than architectural lighting, and along with isoPPFD plots clearly indicate whether the uniformity is acceptable for consistent crop yield.

This report does not consider plant factories with a single layer of plants, such as cannabis production. In this situation, the walls and ceiling should ideally be painted white to maximize reflected light that will improve lighting uniformity. Again however, calculating the light uniformity during the design stage will avoid potential expensive situations once the installation has been completed.

Finally, it should go without saying that accurate predictions of lighting uniformity are only possible with careful measurements of the photosynthetic photon flux intensity (PPI) distributions of the luminiares and careful use of lighting design software to model the application.

ACKNOWLEDGEMENTS

All greenhouse and vertical farm lighting calculations presented in this report were generated with SunTracker Technologies' *CERISE365+GREENHOUSEDESIGNER* horticultural lighting design software (www.heliosolsoft.com).

REFERENCES

Armstrong, J. D. 1990. “A New Measure of Uniformity for Lighting Installations,” J. Illuminating Engineering Society 19(2):84-89.

Both, A. J., et al. 2002. “Evaluation of Light Uniformity Underneath Supplemental Lighting Systems,” Acta Horticulturae 580: IV International Symposium on Artificial Lighting. DOI: 10.17660/ActaHortic.2002.580.23.

CEN. 2002. Light and Lighting – Lighting of Work Places – Part 1: Indoor Work Places, EN 12464-1. European Committee for Standardization.

Ciolkosz, D. E., et al. 2001. “Selection and Placement of Greenhouse Luminaires for Uniformity,” Applied Engineering in Agriculture 17(6):106-113. DOI: 10.13031/2013.6842.

Eaton, M. 2021. “Light Simulation in Greenhouses,” GLASE Technical Article Series Issue 8. https://glase.org/technical-articles/light-simulation-in-greenhouses/.

Ewing, J. L. 1979. “The Price of Uniformity,” J. Illuminating Engineering Society 9(1):47-52.

Ferentinos, K. P., and L. D. Albright. 2005. “Optimal Design of Plant Lighting Systems by Genetic Algorithms,” Engineering Applications of Artificial Intelligence 18(4):473-484. DOI: 10.1016/j.engappai.2004.11.005.

Houser, K. W., et al. 2011. “Illuminance Uniformity in Outdoor Sports Lighting,” Leukos 7(4):221-235.

IES. 1947. IES Lighting Handbook: The Standard Lighting Guide. New York, NY: Illuminating Engineering Society.

Mahdavi, A., and V. Pal. 1999. “Towards an Entropy-based Light Distribution Uniformity Indicator,” J. Illuminating Engineering Society 28(1):24-29.

Marcelis, L. F. M, et al. 2006. “Quantification of the Growth Response to Light Quantity in Greenhouse Grown Crops,” Acta Horticulturae 711:97-104.

Mathieu, J.-P. 1989. “Statistical Uniformity: A New Method of Evaluation,” J. Illuminating Engineering Society 18(2)L 76-80.

Ngai, P. Y. 2000. “The Relationship between Luminance Uniformity and Brightness Perception,” J. Illuminating Engineering Society 29(1):41-50.

Ponce, P., et al. 2015. Greenhouse Design and Control, p. 45. Leiden, The Netherlands: CRC Press.

Runkle, E. 2017. “The Importance of Light Uniformity,” Greenhouse Product News, March, pp. 38.

Thomas, J., and I. Ashdown. 2022c. “Daily Light Integral Distributions: Geographic Similarity,” ISHS Acta Horticulturae 1337, International Symposium on Light in Horticulture, pp. 265-270

Yao, Q., et al. 2017. “Evaluation of Several Different Types of Uniformity Metrics and their Correlation with Subjective Perceptions,” Leukos 13(1):33-45.

Yelton, M., et al. 2017. “Creating Light Uniformity in the Greenhouse,” 2017 ASHS Annual Conference (https://ashs.confex.com/ashs/2017/webprogramarchives/Paper27204.html).

A NEW IES STANDARD BLOOMS

Ian Ashdown, Senior Scientist of SunTracker Technologies has contributed to RECOMMENDED PRACTICE: HORTICULTURAL LIGHTING Published on IES Website and referred to in LD+A Magazine 2022/04/06

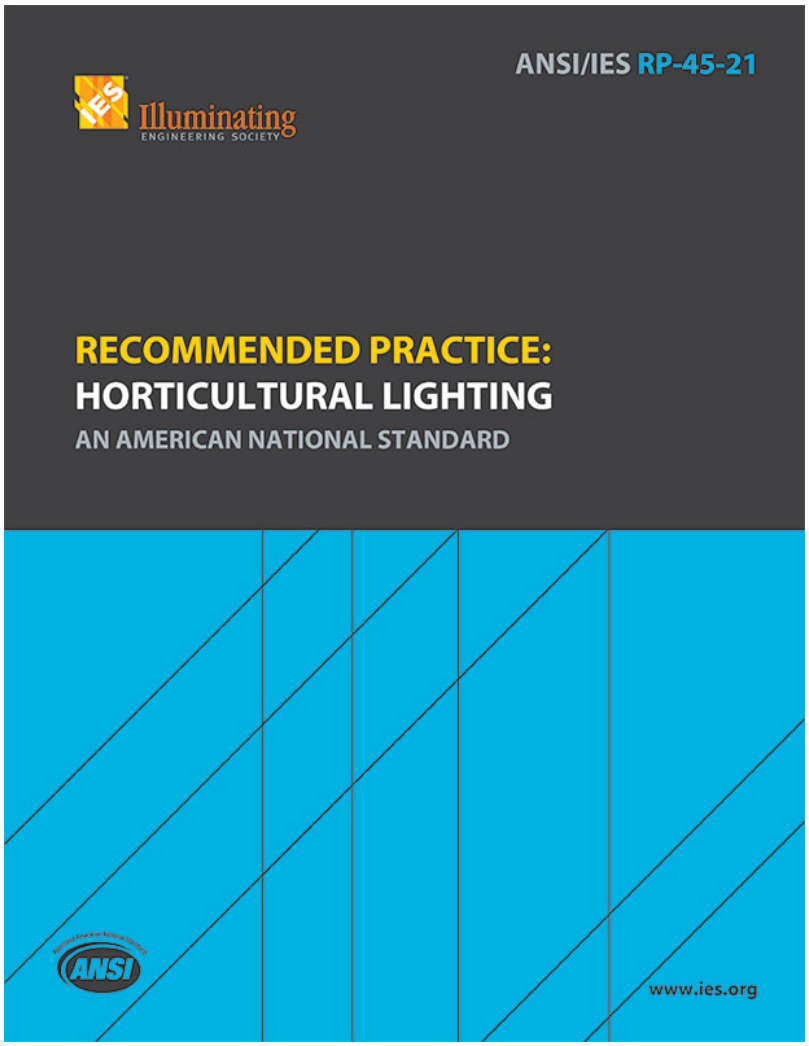

ANSI/IES RP-45-21, Recommended Practice: Horticultural Lighting

The IES has introduced ANSI/IES RP-45-21, Recommended Practice: Horticultural Lighting, to describe the differences between architectural and horticultural lighting design. Included in the Lighting Applications Standard Collection and published in consensus by the IES Horticultural Lighting Committee, the document is paramount for lighting professionals interested in designing atria, greenhouses and indoor farms. Horticultural Lighting Committee Chair Ian Ashdown explains, “Horticultural lighting is a science in its own right—bridging horticulture, botany and illumination engineering. We wrote this document with one purpose in mind: to provide a framework for discussions between horticulturalists and lighting professionals.” To learn more, visit store.ies.org.

LIGHTING DESIGN AS A CROSS-DISCIPLINARY SCIENCE

https://www.led-professional.com/lpr-magazine March/April 2022 (p8)

What does the *metaverse*, the promised "next chapter for the Internet" (Mark Zuckerberg, 2021), have to do with architectural lighting? It will be after all an immersive virtual world where people will gather to socialize, play, and work.

The first and obvious answer is that the metaverse will be a reflection of our physical world, where companies will want their virtual storefronts and gathering spaces to be as engaging as their physical counterparts. This will give professional lighting designers the opportunity to design lighting for virtual spaces in much the same manner as we do now with lighting design software for physical spaces.

We can do better, however. The second and more subtle answer lies in what we already know about the psychophysics of spatial and temporal human vision. There is a much richer and more rewarding set of opportunities and challenges for start-up companies that may come from applying this knowledge.

Think about it: the metaverse will be nothing more than the projection of images onto the viewer's retinae. With eye tracking technology, we will know the viewer's gaze direction and hence the spatial distribution of cones, rods, and ipRGCs onto which the images are being projected. From vision and color science, we already know that our perception of reality can be influenced by what our retinae see and how our visual cortex processes the flow of information – we can manipulate this information frame-by-frame to our advantage.

The knowledge is there for all to see, published in peer-reviewed academic journals. What is often not there, however, is an understanding of how it can be applied to lighting design, or more specifically to how we perceive our environment through optical radiation. To apply this knowledge, we need to thoroughly understand the topic from our perspective.

Speaking more generally, lighting design is inherently a cross-disciplinary science. Think, for example, of circadian-based lighting, light pollution, light-based communications, Internet of Things, ultraviolet germicidal disinfection, and horticultural lighting. We invariably ask, "How can I apply existing products and technologies to these market opportunities?"

This is however precisely the wrong question. We should instead ask, "What is *missing* here?" To answer this question, we ourselves need to become experts in the specific field, whether it is circadian rhythms, light pollution, virology, or botany. We do not need to understand every detail, but we do need to understand how the field relates to optical radiation. Only then will we see the true opportunities and challenges related to lighting, even though they may not be evident to acknowledged experts in the field.

Take for example horticultural lighting and its relation to botany. Should you as a lighting entrepreneur care about the spectral and temporal responsivity of the photopigment phytochrome in relation to the end-of-day responses of plants, and in particular diurnal and circannual changes in atmospheric sky color? If you want to be on the cutting edge of lighting technology, the answer is unequivocal: yes.

Horticultural lighting is not about using blue InGaN and red AlInGaP LEDs to maximize photosynthesis; it is about manipulating the spectral and temporal properties of light sources to optimize the multidimensional aspects of plant growth and development. From the molecular underpinnings of plant photomorphology and (in this case) atmospheric physics, we need to look well beyond lighting science.

The same principle applies everywhere that lighting of any sort has an impact: the opportunities and challenges come from fully understanding the potential scope of the application. It is not about how we illuminate something, but how that something responds to and utilizes light.

Ian ASHDOWN

Ian Ashdown is cofounder of the All Things Lighting Association (ATLA), a non-profit organization whose purpose is to advance, support, promote and contribute to innovation, science, and engineering in lighting, including lighting for health, horticulture, architecture and entertainment.

He is also President and Senior Scientist for SunTracker Technologies Ltd., where he develops lighting design and analysis software for horticulture, architecture, entertainment, and ultraviolet germicidal disinfection. He has been doing lighting research for thirty years, and currently holds 75 patents in many fields of lighting science and technology.

https://www.led-professional.com/lpr-magazine

HEALTH INFORMATION

MODELING SPHERICAL IRRADIANCE FOR UV-C AIR DISINFECTION

Ian Ashdown, P. Eng., FIES, Senior Scientist, SunTracker Technologies Ltd. Published: 22/05/20

We have been using ultraviolet radiation as a means of disinfection for over a century. However, it has been the unfortunate events of the past year that have led to an explosion of interest in ultraviolet germicidal irradiation (UVGI) systems. From mercury vapour and pulsed xenon lamps to excimer lamps and ultraviolet LEDs, there have been, and continue to be, remarkable advances in ultraviolet radiation technology.

What we have yet to see, however, are comparable advances in our ability to model, and more importantly analyze the performance of, UVGI systems.

Architectural lighting designers have had the ability to model and analyze their designs for over fifty years. Using measured luminous intensity distributions provided by the luminaire manufacturers and architectural CAD models provided by their clients, they can quickly model the distribution of surface illuminance, taking into account both direct illuminance from the light sources and indirect illuminance due to interreflections from the environment surfaces.

Now, it is a straightforward process to adapt architectural lighting design software to UVGI applications. After all, both ultraviolet radiation and visible light are optical radiation that obey the same physical laws of optics. One of the advantages of doing this is that it becomes possible to predict the irradiances of surfaces that are hidden from direct view of the radiation sources. In Figure 1, for example, a mobile UV-C platform is being used to disinfect an operating theatre.

UVGI DESIGN SOFTWARE

It is also possible to model the UV-C dose, or *FLUENCE*, of surfaces by considering multiple positions and dwell times for the mobile platform. Intelligent UV-C robots can be programmed to determine an optimal path for room disinfection. Using UVGI design software, it is possible to identify surfaces that may not receive a sufficient dose, and so flag them for enhanced terminal cleaning.

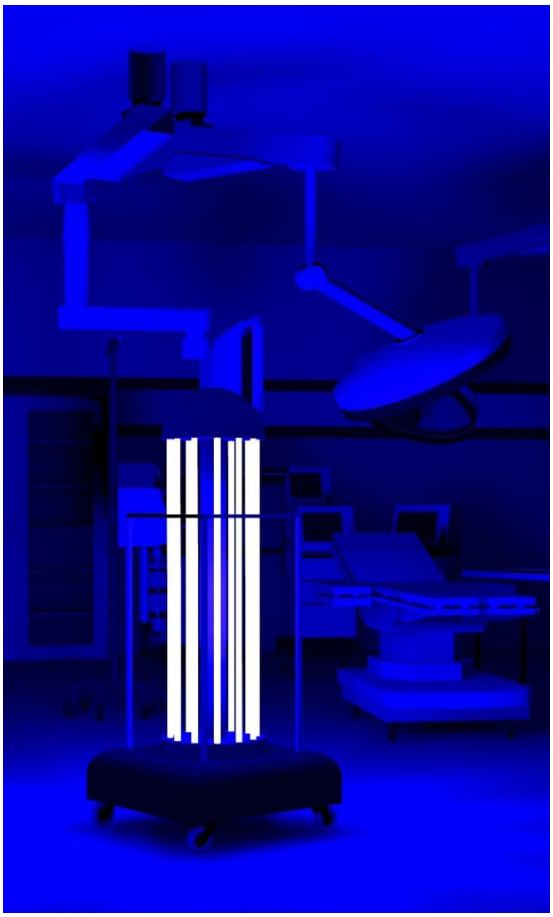

FIG. 1 – Mobile UV-C platform disinfecting a surgical operating theatre.

At the beginning of the COVID-19 pandemic when we were being advised to disinfect every surface, UVGI design software like this made perfect sense. However, we have known for over eighty years that aerosols are the primary transmission vector of respiratory diseases such as tuberculosis, measles, and influenza. Why it took nearly a year to acknowledge that this is also true for coronaviruses is a mystery, but the focus is now on the disinfection of air for interior spaces. This opens the door for the widespread adoption of UVGI systems using low-pressure mercury vapour lamps, ultraviolet-emitting LEDs, and far-UV excimer lamps.

We have, and are continuing to develop, the technology, but how can we model its performance? In particular, how can we model the spatial distribution of ultraviolet radiation in a volume of air?

SPHERICAL IRRADIANCE

We begin with a few definitions. Surface *IRRADIANCE* refers to the radiant power per unit area incident on a surface, regardless of the direction the radiation is coming from (Figure 2). For UVGI applications, it is measured in microwatts per square centimeter (mW/cm^2).

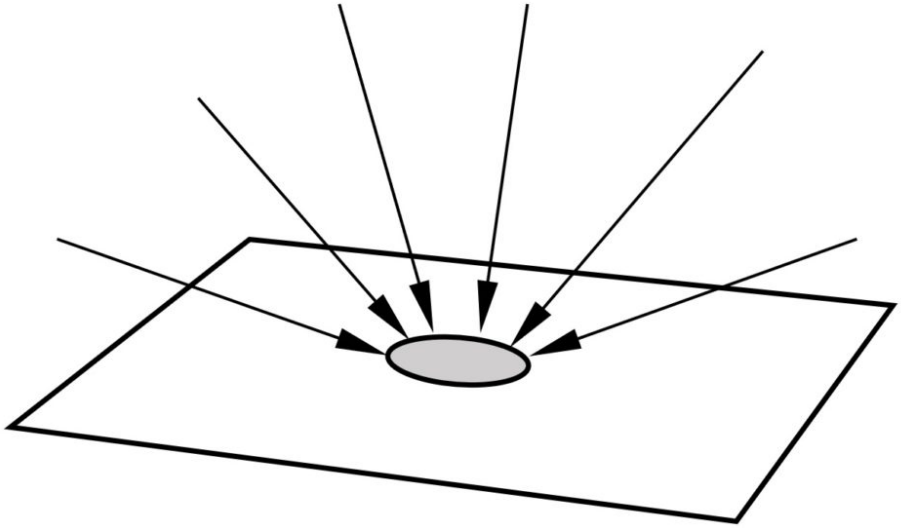

FIG. 2 – Surface irradiance

For aerosols and liquid droplets suspended in air, *SPHERICAL IRRADIANCE* refers to the radiant power per unit area incident on the aerosol droplet from all directions. For any given direction, the area of interest is the cross-sectional area of the spherical droplet. Integrating over all possible directions, we have the spherical irradiance, or *FLUENCE RATE*, of the droplet, also measured in microwatts per square centimeter (Figure 3).

It is important to note that these definitions consider radiation received both directly from radiation sources, and indirectly from surface reflections. While many common materials have low UV-C reflectances, some materials, for example sheet aluminum, can have reflectances as high as seventy percent.

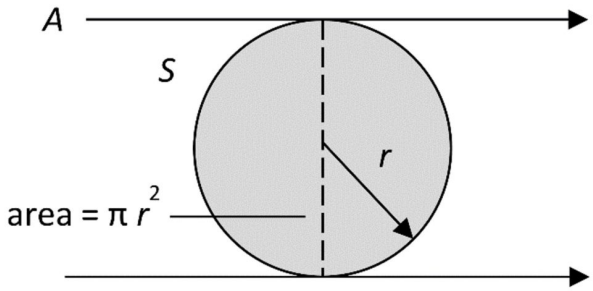

$$E_{e,o} = \int_{4\pi} L_e d\Omega$$

FIG. 3 – Spherical irradiance (fluence rate)

For UVGI applications, we are interested in the ultraviolet dose, or *FLUENCE*, of the droplet, measured in millijoules per square centimeter. Unfortunately, there are no practical instruments to accurately measure ultraviolet fluence, apart from spherical actinometers – hollow quartz spheres filled with photoreactive chemicals such as ferrioxalate in solution.

We are however interested in not measuring, but modeling spherical irradiance in a volume of air, and so we need a virtual spherical irradiance (SI) meter.

VIRTUAL SI METERS

From a mathematical perspective, it is easy enough to model the performance of spherical actinometers. However, the mathematics of spherical geometry are complex and difficult to solve in a reasonable amount of time. Moreover, we will need hundreds to thousands of spherical irradiance meters to model large volumes of air in complex architectural environments.

The solution is to replace the sphere with a six-sided dual cubic tetrahedron – imagine two three-sided pyramids mounted base-to-base (Figure 4). Like the sphere, each face will receive direct and indirect irradiance from its surrounding environment. Fortunately, the planar faces result in a much simpler mathematical model. This will allow us to position a three-dimensional array of meters in the virtual space in order to sample its ultraviolet radiation field.

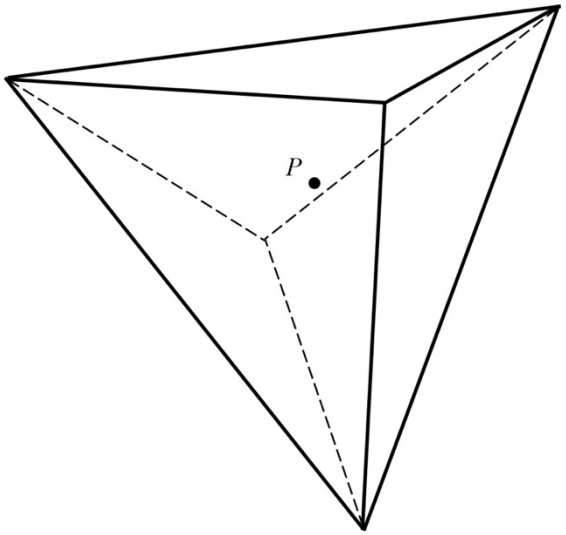

FIG. 4 – Dual cubic tetrahedron

The calculation procedure is both simple and fast. Each dual cubic tetrahedron face is subdivided into a triangular array of elements, much like a computer display consists of a rectangular array of pixels (Figure 5). If we imagine being at the center of the meter, we have a 360-degree spherical view of the environment. In theory, we cannot tell whether we are viewing the actual environment or looking at six triangular computer displays surrounding us.

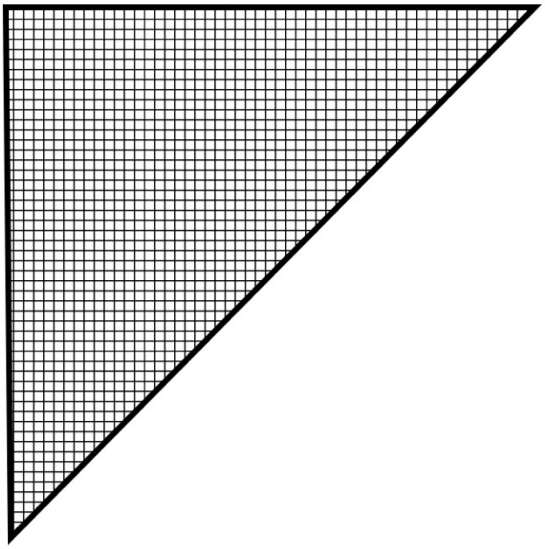

FIG. 5 – Subdivision of cubic tetrahedron face.

With this, we can project each visible object (or portion thereof for partially-hidden objects) onto the faces (Figure 6). This allows us to calculate the irradiance received from each visible object, and to sum the results to obtain the spherical irradiance.

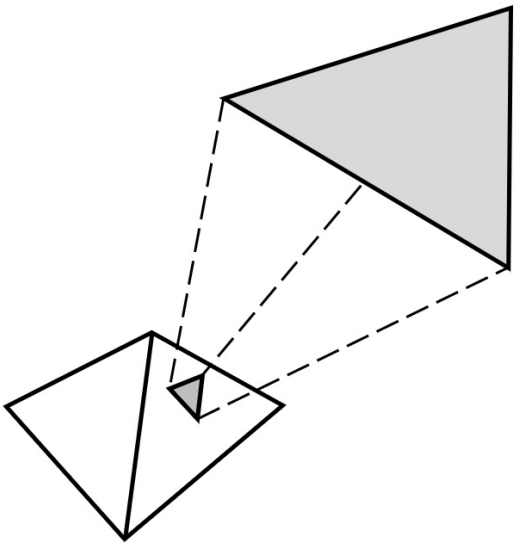

FIG. 6 – Project object onto face.

This is only a conceptual outline of the virtual spherical irradiance meter design. The design itself is based on radiative transfer theory, referred to in computer graphics research as “radiosity.” Developed in the 1980s for architectural visualization, it is fully applicable to UVGI modeling. (Today, the radiosity method forms the basis of Lighting Analysts’ *AGI32* and *ELUMTOOLS* architectural lighting design software.)

The key point here is not the implementation of the meter design, but its speed. Using a desktop computer, it takes only seconds to minutes to model thousands of spherical irradiance meters in complex environments.

Virtual spherical irradiance meters have a variety of applications, including the modeling of air disinfection systems. In Figure 7 for example, air flows through the serpentine channel of a recessed T-grid air sanitizer while being exposed to ultraviolet radiation emitted by seventy-two LEDs. From a design perspective, the average spherical irradiance within the channel is strongly dependent on the reflectance of channel walls. Modeling the system allows us to optimize the design.

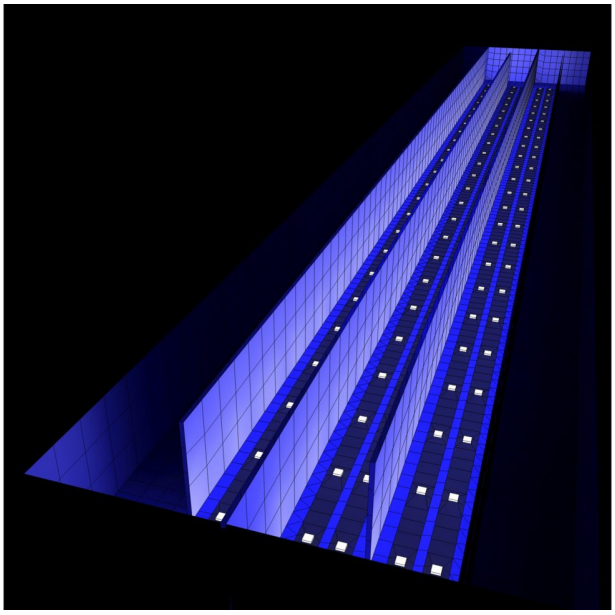

FIG. 7 – Recessed T-grid air sanitizer design

Using CAD modeling, it is easy to represent even the most complex air-handling unit (AHU) geometries with their ultraviolet disinfection lamps (e.g., FIG. 8). Again, the spherical irradiance distribution within the units can be sampled with arbitrary density using a three-dimensional array of spherical irradiance meters.

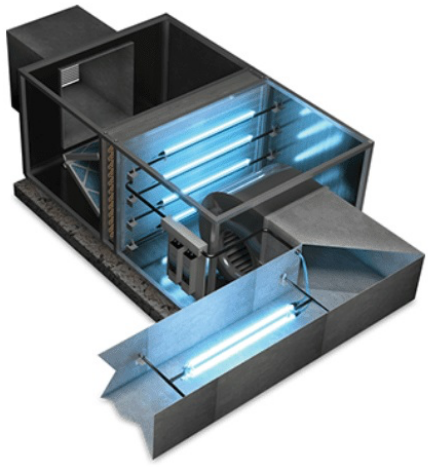

FIG. 8 – Air-handling unit with UV-C disinfection lamps. Source: www.freshaireuv.com.

The problem however is that the air flow within most air-handling units is turbulent. It is not the fluence rate that is important in deactivating pathogens, but the fluence. Turbulence affects how long the aerosols remain in the irradiance field, and so it must be accounted for in predicting the effectiveness of air disinfection.

COMPUTATIONAL FLUID DYNAMICS (CFD)

To address this issue, it may therefore be necessary to employ computational fluid dynamic, or "CFD," techniques to predict the time-averaged air flow through the air-handling unit (e.g., Figure 9). The predicted static irradiance field provides an input to any commercial or open-source CFD program.

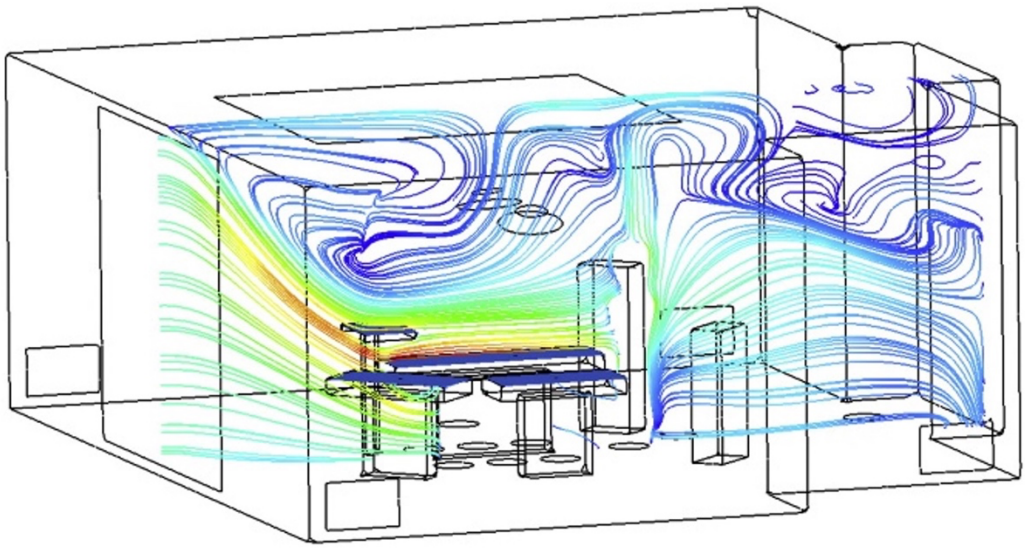

Figure 8 – Computational fluid dynamic modeling of air flow in an operating theatre. Sadrizadeh, S., and S. Holmberg. 2014. "Surgical Clothing Systems in Laminar Airflow Operating Room: A Numerical Assessment," J. Infection and Public Health 7(6):508-516.

Unfortunately, mechanical engineers rarely employ CFD techniques when designing air handling systems for entire rooms, let alone complex architectural spaces such as hotel lobbies and theatres. Instead, building codes simply specify minimum air changes per hour.

This however will undoubtedly change in response to the current COVID-19 pandemic. Studies of infections in restaurants and other situations have highlighted the importance of differential air flow within enclosed spaces, and building codes will need to be revised to address this issue.

To summarize, it is possible to adapt existing architectural lighting design software to predict the ultraviolet irradiance of surfaces in complex environments, including both direct and indirect radiation. However, modeling air disinfection requires virtual spherical irradiance meters to be implemented within this software.

This article has outlined a novel approach that enables thousands of spherical irradiance meters to densely sample large volumes of air in these environments. The calculation times range from seconds to minutes, making the approach ideal for modeling air disinfection systems, air-handling units, upper-room applications with UV-C, and whole-room applications with far-UV.

Spherical irradiance meters are part of the solution in that they can predict fluence rates within air volumes. However, due to air flow turbulence in complex environments, computational fluid dynamic calculations will be needed to model the fluence that any aerosols may be exposed to.

Regardless, virtual spherical irradiance meters enable the modeling of UVGI systems. With them, we can design safe and effective air quality systems for the post-pandemic era.

VISIBLE LIGHT DISINFECTION

Ian Ashdown, P. Eng., FIES, Senior Scientist, SunTracker Technologies Ltd. Published: 22/05/19

Visible light disinfection is a lighting industry innovation wherein violet light is claimed to inactivate pathogens such as bacteria and viruses. Unlike germicidal lamps emitting ultraviolet-C radiation, visible light does not pose the considerable risks of photokeratitis ("snow blindness") and erythema ("sunburn") for room occupants. With the availability of inexpensive and efficient violet LEDs, the technology is being adopted by major luminaire manufacturers for everything from hospital operating theatres to residential kitchens.

As is often the case with new and exciting technologies however, the marketing efforts of both large and small manufacturers sometimes exceed the bounds of scientific evidence. For example, one manufacturer is currently claiming that its products are "… scientifically proven to kill 94% of SARS-CoV-2 under a range of conditions," without any reference to the academic literature in support of this claim.

Other manufacturers are referencing peer-reviewed medical literature in support of their product claims, but the details can be frustratingly vague. For example, Murrell et al. (2019) reported a study of the efficacy of visible light disinfection in operating theatres wherein the manufacturer of the luminaires "… provided technical assistance before and during installation to ensure that proper illumination and disinfecting dose was achieved across the entire OR." Unfortunately, the authors provided no indication of what the disinfecting dose (irradiance times exposure period) was.

From an engineering perspective, this is more than frustrating; it is irresponsible. If a professional lighting designer were to be asked to design or specify a visible light disinfection system in any setting, it would be the designer's responsibility to understand both the benefits and risks of the technology, and to ensure that the target irradiance levels and operating conditions are appropriate. This presents

a problem in that there are as yet no lighting or healthcare industry standards, or even guidelines, for designers to follow. (This may be contrasted with ongoing work by the ASHRAE, IEC, IES, IUVA, and other organizations to develop ultraviolet radiation standards and recommended practices.)

ANCIENT AND MODERN HISTORY

Despite appearances, visible light disinfection is by no means a new technology. The ancient Egyptians reported the health benefits of sun exposure some six millennia ago, while ancient Greek, Roman and Arabic cultures similarly recognized the therapeutic values of sunlight (e.g., Aldahan 2016). The benefits of phototherapy (or more specifically heliotherapy) were given scientific support by Downes and Blunt (1877), who reported that bacteria were inactivated by sunlight, and that violet-blue light was the most effective.

Ward (1894) quantified this antibacterial effect by dispersing sunlight with a prism and projecting it onto an agar plate with anthrax bacteria (*BACILLUS ANTHRACIS*) colonies. The inhibition of colonies (FIG. 1) clearly demonstrated the action spectrum of sunlight, showing that blue light (B) was the most effective.

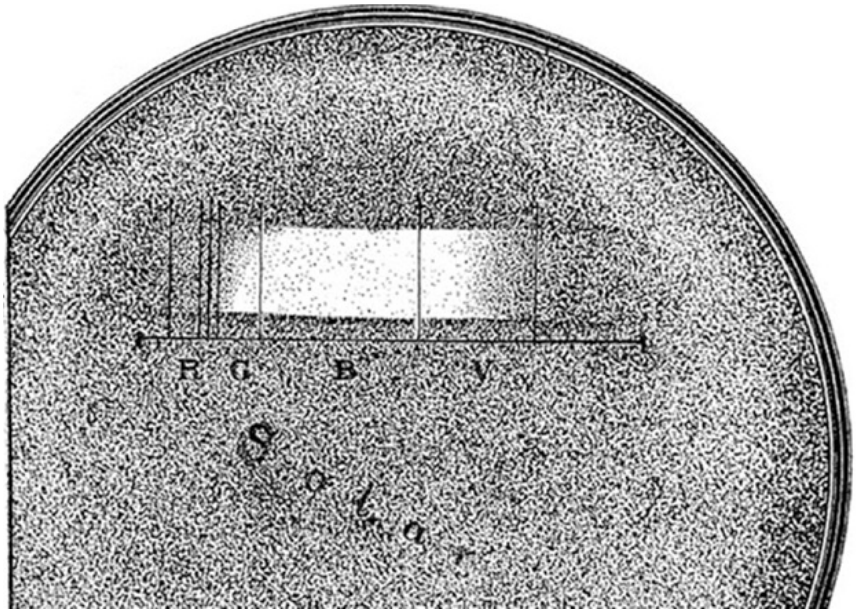

Figure 1 – Bacterial inhibition of anthrax colonies of agar plate using sunlight (Ward 1894).

The work of Downes and Blunt inspired Niels Finsen, a Danish medical researcher, to investigate further. After initial experiments in the early 1890s with natural light, he developed an apparatus using electric carbon arcs that would later become known as the “Finsen light” (Grzybowsky and Pietzrak 2012).

Figure 2 – Niels Ryberg Finson (1860 – 1904). Source: Wikipedia.

Finsen began his experiments using common glass lenses to focus the electric arc emission, but knew from the work of Ward (1894) and others that ultraviolet radiation was germicidal, and so he replaced these lenses with fused quartz. However, as reported by Møller et al. (2005), Finsen used methylthioninium chloride ("methylene blue") in solution as a heat-absorbing filter. Likely unknown to Finsen, this dye absorbs ultraviolet radiation with wavelengths shorter than 340 nm. The Finsen light therefore produced ultraviolet-A radiation and visible light, but no germicidal ultraviolet-B radiation.

Regardless, use of the Finsen light as a treatment for lupus vulgaris (a painful skin infection caused by *MYCOBACTERIUM TUBERCULOSIS*) was an astounding success. Between 1886 and 1901, the Finsen Institute treated 804 patients, of whom 83 percent were cured (FIG. 3). For this work, Finsen received the 1903 Nobel Prize in Medicine and Physiology. The science of phototherapy was (re)borne.

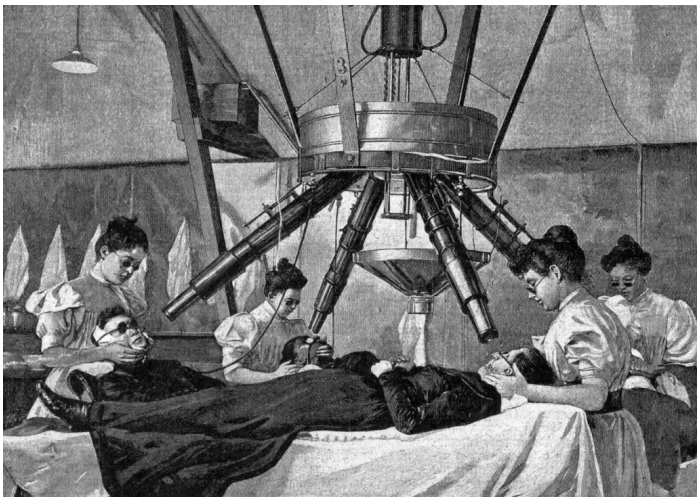

Figure 3 – Finsen light being used to treat lupus vulgaris patients circa 1900. Source: Wikipedia.

HOW IT WORKS

Germicidal lamps, including low-pressure mercury vapour arc lamps emitting 254-nm UV-C radiation, Kr-Cl* excimer lamps emitting 222-nm UV-C radiation, and LEDs emitting narrowband UV-B or UV-C radiation, work by disrupting the DNA of bacterial and fungal spores, and the DNA or RNA of viruses. This disables the cellular mechanisms of bacterial and fungal spores, thereby inactivating them, and prevents viruses from being able to replicate.

Visible light is different in that the individual photons do not have sufficient energy to disrupt DNA or RNA. Bacteria, fungi, and protozoa contain intracellular (endogenous) porphyrins that strongly absorb visible light in a region of the spectrum called the Soret band (e.g., Figure 4).

These photosensitizers consequently transfer the photon's energy to an oxygen molecule within the cell, producing a "reactive oxygen species" (ROS) molecule, such as singlet oxygen or hydrogen peroxide, that is highly reactive and cytotoxic (e.g., Kumar et al. 2015, Ramakrishnan et al. 2009). It is the ROS that inactivates the cell by disrupting its cellular machinery (e.g., Plavskii et al. 2014).

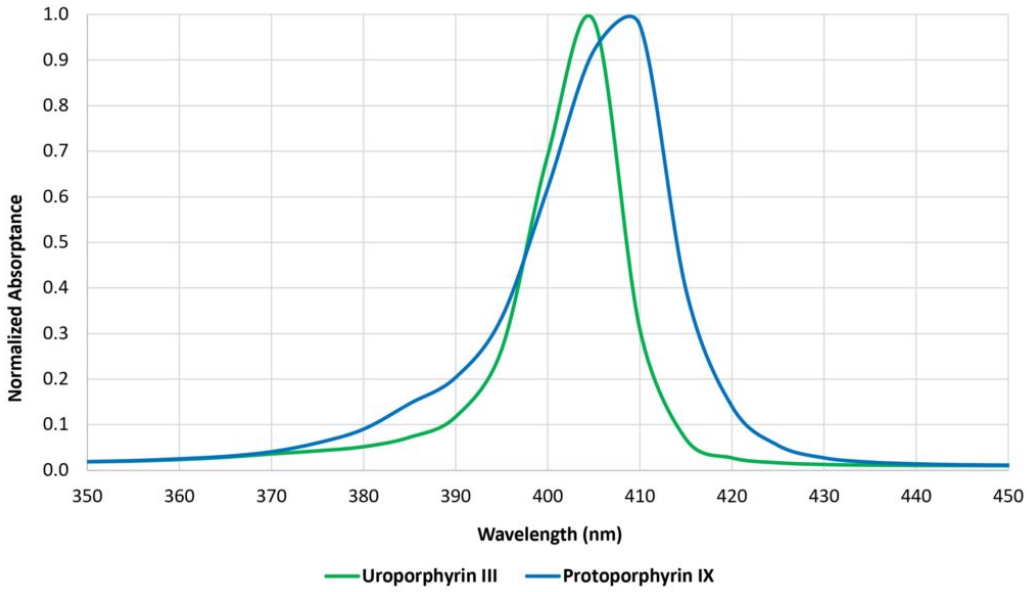

Figure 4 – Porphyrin absorptance spectra (normalized). Adapted from Hessling et al. 2017.

It must be said however that this is the prevailing theory; there is evidence for other explanations of how visible light inactivates pathogens, including different photosensitizers such as riboflavin acting at 450 nm (e.g., Hönes et al. 2018, Tomb et al. 2018) and different cellular inactivation mechanisms (e.g., Tomb et al. 2018, Halstead et al. 2019).

Viruses are different in that, unlike bacteria, fungi, and protozoa, they do not contain porphyrins and so in theory should not be susceptible to blue light. Nevertheless, there is growing evidence that they may be. This will be discussed below under "Viruses and Bacteriophages."

The germicidal effects of visible light have been demonstrated for wavelengths from approximately 380 nm to 740 nm, but peak efficacy has been demonstrated at approximately 405 nm (e.g., Maclean

et al. 2008, Hessling et al. 2017, Tomb et al. 2018). This is therefore the nominal wavelength employed by commercial visible light disinfection products (e.g., Rutula et al. 2018).

Various photosensitive drugs (exogeneous photosensitizers) are used in photodynamic therapy, wherein the drugs are absorbed by the diseased cells and then activated by exposure to visible light. The resultant ROS then elicit cell inactivation in the diseased tissue. Typical applications include treatment of acne, macular degeneration, psoriasis, atherosclerosis, and malignant cancers (e.g., Hamblin and Hasan 2004). This topic is relevant to visible light disinfection in that the US Federal Drug Administration may choose to regulate the use of 405 nm light as a potential photosensitizer, particularly in hospitals where patients may be on drugs with known photosensitizing effects.

Visible light disinfection, then, has a firm scientific basis for medical applications. However, its usefulness in disinfecting enclosed architectural spaces, from hospital operating theaters to residential kitchens, is considerably more nuanced. The remainder of this article therefore focuses on the many factors that must be considered when evaluating, or designing with, visible light disinfection products for various applications.

IRRADIANCE AND DOSE

Knowing how visible light disinfection works does not answer the question: what irradiance and dose of visible light are needed to achieve satisfactory results? It is difficult to find relevant information, even in the many medical papers that have been published over the past fifteen years or so.

The first step is to define our terms of measurement. Irradiance, measured in milliwatts per square centimeter (mW/cm^2), is the radiant equivalent of illuminance (which can be measured in lumens per square centimeter). Dose may be a less familiar concept to lighting designers, but it is the irradiance multiplied by the exposure time in seconds, expressed in joules (i.e., watt-seconds) per square centimeter (J/cm^2). It is the radiant equivalent of luminous energy, but we never have a need to consider this unit in lighting design.

The next step is to understand what it means to “inactivate” pathogens in a practical sense. When exposed to constant irradiance, whether it is visible light or ultraviolet radiation, the rate of inactivation is initially exponential. That is, if 90 percent of the pathogens are inactivated after (say) one hour, 90 percent of the surviving pathogens will be inactivated after another hour. Thus, there will be 90 percent inactivation after one hour, 99 percent after two hours, 99.9 percent after three hours, and so on.

It is often more convenient to express these numbers in $\log_{10}$ (“log-ten”) units, where one $\log_{10}$ unit represents 90 percent inactivation of the initial number of pathogens, two $\log_{10}$ units represents 99 percent, three $\log_{10}$units 99.9 percent, and so on. (Another term for $\log_{10}$ units is “D-value.”)
The desired degree of disinfection will depend on the application. For example, the US Food and Drug Administration (FDA) requires sterilized surgical instruments to have D-values of six or greater (99.9999 percent inactivation), on the assumption that the remaining pathogens are too few in number to cause infections. For visible light disinfection however, it is common to specify 90 percent, or one $\log_{10}$, inactivation.

Reducing the number of pathogens by 90 percent may not seem particularly useful, but it must be remembered that visible light disinfection, like ultraviolet-C disinfection in a hospital, should always be considered as a supplement to terminal cleaning. Its primary purpose is not to eradicate existing bacterial colonies, but basically to prevent those colonies from growing before the next terminal cleaning.

SPECIES AND STRAINS

Some luminaire manufacturers list numerous pathogens that are susceptible to their products, with names like *STAPHYLOCOCCUS AUREUS*, *LISTERIA MONOCYTOGENES*, *SALMONELLA ENTERITIDIS* … the list goes on. Fewer than one hundred bacteria species have been examined for visible light susceptibility, and even fewer fungi and viruses. Even among this select group of common pathogens, however, the range of visible light doses needed to achieve 90 percent inactivation can be enormous (Fig. 5). For example, different strains (i.e., genetic variants) of methicillin-resistant *STAPHYLOCOCCUS AUREUS* (MRSA) may need between 13.7 and 1200 J/cm, depending on the laboratory conditions(e.g., Tomb et. al. 2018). In general, observed dose differences for single species of up to one order of magnitude may be expected from different laboratory studies, with fungi and viruses requiring considerably higher doses than most bacteria (Hessling et al. 2017, Tomb et al. 2018).

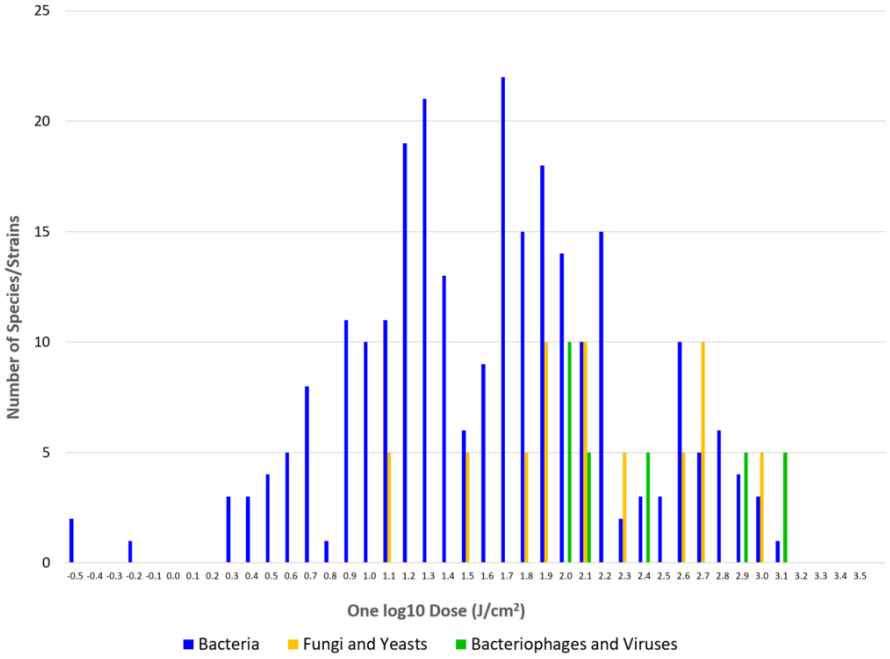

Figure 5 – Range of one $\log_{10}$ doses of 405-nm radiation for 90 pathogen species. Adapted from Tomb et al. 2018.

For test purposes, pathogens can be grown as colonies on growth media in Petri dishes or in solution, or nebulized (i.e., aerosolized) for airborne species. Their susceptibility to visible light may depend on the irradiance, the exposure time, the relative humidity, the growth medium, oxygen concentration, density (expressed in colony-forming units per milliliter, or CFU/ml), and the pathogen strain.

It gets worse: when a paper reports a given irradiance, it could be due to a single LED with a range of 10:1 over the irradiated area. For LED arrays, the irradiance could be measured at the sample surface or the LED diffuser plate (Dai et al. 2012). The transparent Petri dishes could be placed on a reflective

base, which could increase and possibly double the irradiance the pathogens receive due to reflected light (Bumah et al. 2013, Hessling et al. 2017). Growth medium additives can include phenol red, which strongly absorbs in the blue/violet region of the spectrum (Hessling et al. 2022a). This makes it difficult to compare studies of minimum dose needed to achieve one $\log_{10}$ inactivation.

This problem is not limited to visible light disinfection. Freeman et al. (2022) discussed the issues involved in coronavirus disinfection using UV-C, noting that recommended doses ranged from 0.6 to 11,754 J/cm^2. Quoting from their paper, "It highlights a substantial need to standardize a testing platform in order to evaluate germicidal inactivation doses while at the same time to understand how environmental factors influence the inactivation doses for a given pathogen."

BIOFILMS

To further complicate matters, bacteria may form biofilms on surfaces to protect themselves from desiccation, antibiotics, the host body's immune system, and other environmental factors. Biofilms are prevalent in nature, including hospitals and residences. The films themselves are not alive, but they may protect the bacteria from being inactivated by ultraviolet radiation, particularly 222-nm UV-C. (One of the arguments in favor of far-UV is that the short wavelengths are unable to significantly penetrate corneal and skin cells to cause DNA damage. The same argument presumably applies to organic biofilms.) However, McKenzie et al. (2013), Halstead, (2019b), and Huang et al. (2022) report that 405nm visible light is an effective treatment for some bacteria species encapsulated in biofilms.

BLUE LIGHT RESISTANCE

In any microbial population, there will be a tiny fraction that are unusually resistant to UV radiation. Once 99 percent of the population has been inactivated, it is not uncommon for the rate of inactivation to decrease significantly (e.g., Enwemeka et al. 2008, Kowalski 2009). In other words, the surviving pathogens requires higher doses to inactivate them. (The same principle applies to bacteria developing resistance due to the overuse of antibiotic drugs.)

Fortunately, visible light disinfection by design does not generally seek to eradicate microbial populations, but only to limit their growth, or at best achieve 90 percent inactivation. It is therefore unlikely that pathogens will develop blue light resistance, as there is little evolutionary pressure to do so. Indeed, studies with sublethal doses of blue light (e.g., Amin et al. 2016, Tomb et al. 2017a, Leanse et al. 2018) have shown that the bacteria do not develop blue light resistance. However, Guffey et al. (2013) reported a counter-example with *STAPHYLOCOCCUS AUREUS*.

AMBIENT WHITE LIGHT

One issue of concern is that laboratory studies typically isolate the pathogens being studied from environmental factors, including ambient lighting where white light illumination may actively encourage bacterial and fungal colony growth (e.g., Lipovsky et al. 2009). The question is, how should such studies be interpreted in real-world conditions where pathogens are exposed to both violet light for disinfection and ambient white light for illumination? (This is discussed below under "Hospital Settings.")

Some manufacturers are promoting visible light disinfection at irradiance levels where the exposure time is eight hours or more to achieve 90 percent inactivation in the laboratory. If the ambient illumination promotes colony growth, this may reduce the effectiveness of the visible light disinfection.

Hessling et al. (2022b) offer a further data point: using 5600K white light LEDs (which have a very significant peak at approximately 450 nm due to the blue pump LEDs), it required an illuminance of 2,400 lux over 34 hours to achieve a 90 percent reduction of *STAPHYLOCOCCUS SP.* bacteria on glazed stoneware. Adding 2.5 mW/cm^2 of 405 nm irradiation reduced this to 3.5 hours, but the visual appearance of the illumination was well off the Planckian locus and decidedly purplish in color.

VIRUSES AND BACTERIOPHAGES

Whether viruses and bacteriophages (viruses that infect bacteria) are susceptible to visible light is a topic of ongoing research. It has been argued that they should not be because they do not contain porphyrins or other endogenous photosensitizers that are capable of generating ROS. However, viruses examined in the laboratory may be suspended in organically-rich growth media such as fetal bovine serum, which can form ROS (Tomb et al. 2017b, De Santis et al. 2020, Stasko et al. 2021, Hessling et al. 2022a). Also, there may be endogenous photosensitizers in the host cells (Tomb et al. 2014, Rathnasinghe et al. 2021). Alternatively, the host cells may become inactivated due to upregulated production of damaging proteins by bacteriophages (Halstead et al. 2019).
On the other hand, some studies have examined viruses in phosphate buffered saline, which rules out endogenous photosensitizers (Lau et al. 2021, Rathnasinghe et al. 2021, Hessling et al. 2022a).

However, these studies have been mostly limited to enveloped viruses (which include coronaviruses such as SARS-CoV-2), where the visible light is possibly damaging the lipids of the envelopes rather than the virus DNA or RNA.

There is therefore evidence that visible light is capable of inactivating viruses directly, but the reasons are still under investigation. Enwemeka et al. (2021a) and Hessling et al. (2022a) provide excellent summaries. Hessling et al. (2022a) in particular notes that riboflavin in solution may have a major impact on photoinactivation results, and that virus reduction with visible light may require considerably higher doses under other conditions, such as in air. Quoting the authors, “This is especially important in the ongoing corona[virus] pandemic, where frightened citizens seek protective measures and companies might offer deceptive security based on misunderstood studies.”

DIFFERENT WAVELENGTHS

Most visible light disinfection studies conducted to date have focused on the spectral region of 385 nm to 420 nm (Hessling et al. 2017, Tomb et al. 2018). However, bactericidal effects of visible light have been demonstrated with wavelengths of up to 740 nm, as shown in Figure 6 (Hessling et al. 2017). These are presumably due to the absorption characteristics of different endogenous photosensitizers, such as riboflavin around 450 nm (Hönes, K., et al. 2018). However, the dose required for inactivation generally increases exponentially with wavelength.

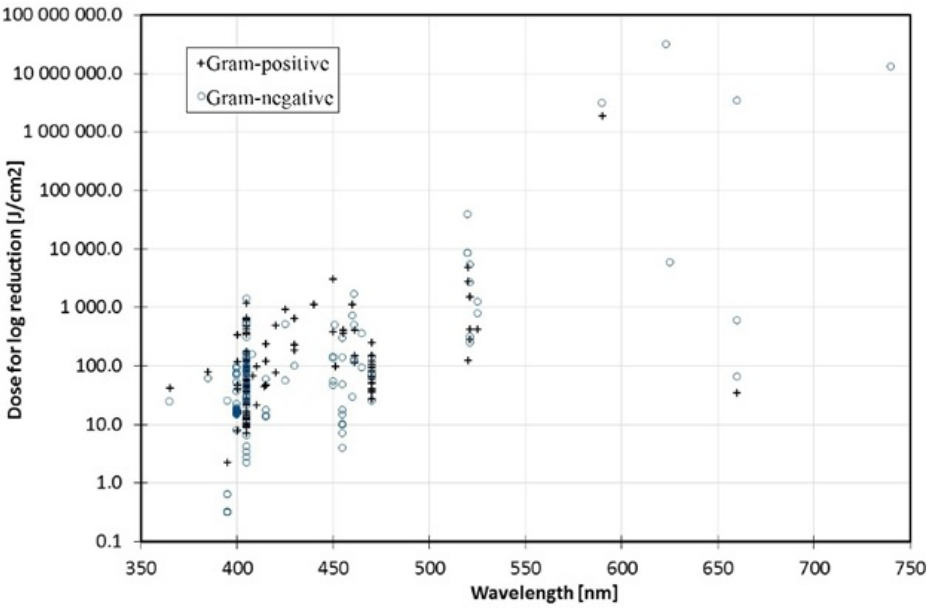

Figure 6 – Bacterial susceptibility versus wavelength. Source: Hessling et al. 2017.

SPECTRAL INTERACTIONS

Most of the studies to date have also focused on narrow spectral bands generated by quasimonochromatic LEDs. One study examined the combination of 405-nm blue light as an antibacterial agent and 880-nm near-infrared radiation as a means of tissue repair, but found that the 880-nm radiation by itself promoted bacterial growth (Guffey and Wilborn 2006). Another study used an array of phosphor-coated white LEDs with both 405 nm and 450 nm peak wavelengths, and with an estimated 6500 K correlated color temperature (CCT), to inactivate SARS-CoV-2 viruses (De Santis et al. 2020). However, the authors acknowledged that the growth medium for the infected cells contained ten percent fetal bovine serum, which may have contributed to the virus inactivation.

In a review titled “Light as a Broad-Spectrum Antimicrobial,” Gwynne and Gallagher (2018) noted that while *ENTEROCOCCUS* bacteria are resistant to blue light, they are sensitive to near- and mid-infrared radiation. Also, *TRICHOPHYTON RUBRUM* fungi (responsible for the fungal infection onychomycosis) are sensitive to green light. The higher dose requirements may preclude these longer wavelengths from practical whole-room visible light disinfection, but more research is clearly required.

PULSED BLUE LIGHT

Several *IN VITRO* studies have investigated the effect of pulsed blue light on the efficacy of visible light disinfection. Gillespie et al. (2017), for example, found that when exposing MSRA bacteria to 116 mW/cm^2 of 405 nm radiation, varying the pulse width duty cycle from 25 to 100 percent had little effect on the dose required to achieve the same degree of inactivation. The pulse width modulation (PWM) frequency was varied from 100 Hz to 10 kHz, with 1000 Hz showing the best performance, and with 35 percent energy savings for a 50 percent duty factor. The authors speculated that the cell porphyrins become saturated with continuous exposure, and that the off period of each cycle enables the absorbed light to generate ROS with fewer photons being absorbed unnecessarily.

Masson-Meyers et al. (2019) similarly found that a duty cycle of 33 percent and a PWM frequency of 33 kHz was optimal for 450 nm radiation treating acne vulgaris caused by the *PROPIONIBACTERIUM ACNES* bacterium. The experiments involved microLEDs mounted on flexible plastic sheets that were applied to the infected skin, but remarkably the required irradiance to achieve 100 percent eradication of the bacteria was 40 to 100 times less than previously reported results for *IN VITRO* experiments involving MSRA bacteria. However, this involved repeated treatments every four hours that were timed to coincide with the replication cycle of *P. ACNES*, as opposed to single exposures of bacterial cultures in the laboratory. Further laboratory experiments with otherwise identical test conditions are likely required to confirm these results.

Bumah et al. (2020) demonstrated that pulsed 450 nm blue light suppresses the formation of MSRA and *PROPIONIBACTERIUM ACNES* bacteria in planktonic cultures and bacterial biofilms. Irradiances of 3mW/cm^2 and three doses of 7.6 J/cm^2 were sufficient to completely eradicate MSRA bacteria in solution, while 2 mW/cm^2 and 5 J/cm^2 were sufficient to eradicate *P. ACNES* bacteria. Assuming that "eradication" means 99.9 percent inactivation, this implies that the doses required for 90 percent inactivation would be 3.8 J/cm^2 and 2.5 J/cm^{2}respectively.

Enwemeka et al. (2021b) demonstrated that pulsed blue with wavelengths ranging from 405 nm to 450 nm inactivated several strains of human coronavirus, but the efficacy varied by strain. Further, the antiviral effect was more pronounced at higher than lower irradiances.

HOSPITAL SETTINGS

Most of the above studies were *IN VITRO* experiments performed in laboratories. This is of course necessary to isolate specific species and strains, and to control or eliminate the influence of environmental conditions such as ambient light and temperature, relative humidity, growth medium, and more.

Investigating the efficacy of visible light disinfection *IN VIVO* under real-world conditions is more difficult, even in hospital settings such as operating theaters and in-patient rooms. Maclean et al. 2010 and Bache et al. 2012, for example, reported on the use of two ceiling-mounted 405 nm LED arrays in burn unit isolation rooms with a floor area of approximately 10 m^2. Unfortunately, the irradiance levels "… were set, on the basis of extensive laboratory experimentation, to be sufficient to cause significant inactivation of exposed bacteria within the room environment" (Maclean et al. 2010). The remainder of the papers were sufficiently detailed, but the lack of irradiance information makes the experiments irreproducible.

Both papers noted that the installations were in compliance with the International Commission on Non-Ionizing Radiation Protection (ICNIRP) guidelines on exposure limits for incoherent visible radiation (ICNIRP 2013). These guidelines however are concerned with light source radiance leading to possible retinal injury; they do not address irradiance levels.

The authors referred to their visible light disinfection unit as a "High-Intensity Narrow-Spectrum light Environmental Decontamination System" (HINS-light EDS). This is useful in that Halstead et al. (2019) later described this device as "a ceiling-mounted LED array which delivers low-irradiance 405-nm light

(irradiance, 0.1 to 0.5 mW/cm^2) continuously to decontaminate surface in hospital operating theaters."

Bache et al. (2012) reported that from over 1,000 environmental samples taken from inpatient isolation rooms and an outpatient clinic, there was a significant reduction in the average number of bacterial colonies (27 to 75 percent) following HINS-light EDS use with 14-hour daily exposures. If we assume an average of 50 percent (0.70 $\log_{10}$) reduction, it would require 20 hours of exposure to achieve 90 percent reduction. Further assuming an average irradiance of 0.3 mW/cm^2, the dose would be 21.6 J/cm^2.

The study involved *STAPHYLOCOCCUS AUREUS*, and referenced Maclean et al. (2008). From this earlier laboratory study, the required dose for 90 percent reduction was 9.8 J/cm^2. While noting that the burn unit rooms had HEPA filters and underwent daily terminal cleaning to minimize the risk of hospital-acquired wound infections, the results were commensurate with what would be expected from laboratory dose requirements.

Maclean et al. (2013) reported on a similar study involving the use of HINS-light EDS units in occupied isolation rooms of intensive care units, but with a focus on the total bacterial contamination around the room rather than just MSRA bacteria. The units were again operated for 14 hours per day in synchrony with hospital lighting. The authors reported an average 50 percent reduction in contamination levels while the units were in use. Moreover, this included indirectly illuminated surfaces within the room, with an approximately 2:1 difference in bacterial reduction.

Bache et al. (2017) continued these studies within the burn unit isolation rooms, finding that there was no correlation between irradiances levels and bacterial inactivation over a range of 0.0023 mW/cm^2 to 0.231 mW/cm^2, but that there was a strong correlation between exposure time (i.e., dose) and bacterial inactivation. The authors attributed this to the bacteria being suspended in air almost indefinitely, which would expose them to higher spherical irradiance levels near the LED arrays due to air movement within the room. Related to this, Dougall et al. (2018) reported that *STAPHYLOCOCCUS EPIDERMIDIS* was three to four more times susceptibility to 405-nm irradiation in aerosol form than when in liquids or on surfaces. This is similar to the susceptibility of most pathogens to UV-C radiation (e.g., Freeman et al. 2022, Kowalski 2009).

This highlights perhaps the most significant difference between ultraviolet radiation and visible light for whole-room disinfection. In most applications, UV-C radiation is used to disinfect air, so that proper air flow is a critical parameter. To date, however, visible light disinfection research has focused on surface disinfection. Studies such as Bache et al. 2017 suggest that visible light may be useful in air disinfection, but there is no conclusive evidence that this is true.

Maclean et al. (2013) further suggest that air disinfection may be involved, as the relatively modest 2:1 difference in bacterial reduction for shadowed surfaces is surprising when irradiance levels under tabletops, for example, are likely five or more times less than exposed surfaces (assuming 20 percent floor reflectance).

Murrell et al. (2019) reported on the successful use of commercial visible light disinfection luminaires in an orthopedic operating room, but did not disclose the irradiance levels. Instead, they stated that,

"The manufacturer provided technical assistance before and during installation to ensure that proper illumination and disinfecting dose was achieved across the entire OR." Again, the lack of irradiance information makes their experiments irreproducible.

Rutala et al. (2018) reported a study involving a 12.5 m^2 windowless room equipped with two 61 cm ´ 61 cm (2-foot square) "blended-white light" LED luminaires and one 61 cm´ 122 cm "blue light" LED luminaire. The white light luminaires provided both disinfection radiation (presumably 405 nm) and "ambient white" light illumination for use in normal clinical applications in an occupied room with an irradiance of 0.12 mW/cm^2 to 0.16mW/cm^2on the pathogen surface, while the disinfecting "blue light" luminaire provided an irradiance of 0.34 mW/cm^2 to 0.44 mW/cm^2.

This study is deficient in that without knowing the spectral power distribution of the luminaires, it is again difficult to reproduce the experiments. Nevertheless, the results shown in Table 1 for 90 percent reduction are informative. The four pathogens are common infectious bacteria in hospitals, but *E. FAECALIS* (responsible for urinary tract infections and meningitis) did not respond to white light, while *C. DIFFICILE* (responsible for a quarter of million hospital infections per year) did not respond to white or blue light at all.

Pathogen	Treatment	Exposure	Dose (J/cm^2)
Staphylococcus aureus	White	24 hr	10.3 – 13.8
	Blue	10 hr	12.2 – 15.8
Enterococcus faecalis	White	N/A	N/A
	Blue	15 hr	18.4 – 23.8
Acinetobacter baumannii	White	14 hr	6.0 – 8.1
	Blue	15 hr	18.4 – 23.8
Clostridium difficile	White	N/A	N/A
	Blue	N/A	N/A

Table 1 – Whole-room disinfection (90 percent) with white and blue light. Source: Rutula et al. 2018.

These results are crucial because they highlight an important issue with visible light disinfection; as shown in Figure 5, the range of doses required for different species and even strains of pathogens are enormous. (Note that the abscissa of Figure 5 is logarithmic.) *CLOSTRIDIUM DIFFICILE* is a spore-forming bacterium that exists in two states: vegetative and endospore. In its vegetative state, it requires a dose of 13 to 77 J/cm^2 for 90 percent reduction; in its endospore state, the dose ranges from 426 J/cm^2 to 736 J/cm^2.

The record holder however is *ASPERGILLUS NIGER*, a common food contaminant that also forms black mold in indoor environments. According to Murdoch et al. (2013), its spores require an astonishing 23,000 J/cm^2 to achieve 90 percent reduction.

SUNLIGHT

As with any new technology, there will be questions concerning potential health hazards. Any commercial visible light disinfection luminaire should of course satisfy the guidelines for retinal safety (ICNIRP 2013), but there are other concerns. In reviewing the safety of violet-blue light exposure, Christensen et al. (2021) reported that exposure to 400 to 500 nm blue light with a dose exceeding 65 J/cm^2 can result in pigment darkening. The authors calculated that with typical indoor light sources, it would require from two weeks to 20 months to reach the threshold dose.

This is somewhat misleading, however. With the sun at zenith on a clear day, the radiant flux in the spectral region of 400 nm to 500 nm is about 14 mW/cm^2(ASTM 2020). The time required to receive a 65 J/cm^2 is therefore about 80 minutes. Still, the authors made a valid observation: visible light disinfection systems may pose a risk to people with photosensitive diseases, or who are taking photosensitizing drugs.

This highlights another issue with visible light disinfection. The health benefits of sunlight have been known for six millennia, and the research referenced here makes it clear why. On a clear day with the sun at zenith, the radiant flux in the Soret band (~390 nm to 420 nm) is about 5 mW/cm^2 (and about 0.5 mW/cm^2 on an overcast day). Over eight hours, this is about 150 J/cm^2.

Simply put, direct sunlight is an excellent visible light disinfectant (not to mention the antimicrobial effects of UV-A and UV-B radiation). Schuit et al. (2020), for example, reported that the half-life (70 percent reduction) of influenza viruses in full direct sunlight is about 150 seconds.

To put this into perspective, 5 mW/cm^2 translates into 500 watts of 405 nm radiant flux for a 10 m^2 (108 square foot) room. If direct sunlight is available, it is a far better choice for visible light disinfection than electric lighting.

WHOLE-ROOM DISINFECTION

As shown by the studies cited in “Hospital Settings,” it is evident that whole-room visible light disinfection systems are useful as a supplement to terminal cleaning in hospital settings. This includes both occupied in-patient rooms with continuous illumination and unoccupied spaces (such as operating theaters) where higher blue light irradiances can be employed. Typical irradiances will be on the order of 0.1 to 0.5 mW/cm^2 (one to five W/m^2), with typical exposure times of 8 to 14 hours to prevent pathogens from proliferating.

It must also be understood, however, that whole-room visible light disinfection systems cannot deliver the irradiances and doses needed to control, let alone eradicate, such common hospital pathogens as *CLOSTRIDIUM DIFFICILE*, let alone the common food contaminant *ASPERGILLUS NIGER*. One luminaire manufacturer currently claims that its products are effective against 26 bacteria, yeast, fungi, and viral species. Referring to Tomb et al. (2018), it is evident that many of these species may require doses for 90 percent inactivation that are far in excess of what practical whole-room visible light disinfection systems can provide.

Pathogen	Species	J/cm² Dose		W/m² (8 hr)*	
		Min.	Max.	Min.	Max.
Bacteria	*Acinetobacter baumannii*	2	26	0.7	9.0
	Bacillus cereus	27	665	9.4	227.4
	Campylobacter jejuni	0.3	3.4	0.1	1.2
	Clostridium difficile	13	736	4.5	255.6
	Clostridium perfingens	10	?	3.5	?
	Corynebacterium striatum	4	64	1.4	22.2
	Enterococcus faecalis	64	410	22.2	142.4
	Escherichia coli	5	612	1.8	212.5
	Klebsiella pneumoniae	16	263	5.6	91.3
	Listeria monocytogenes	17	1121	5.9	389.2
	Mycobacterium terrae	57	?	19.8	?
	Proteus vulgaris	31	?	10.8	?
	Pseudomonas aeruginosa	4	1020	1.4	354.2
	Salmonella enteritidis	72	544	25.0	188.9
	Serratia marcescens	128	337	44.4	117.0
	Shigella sonnei	36	608	12.5	211.1
	Staphylococcus aureus	9	1200	3.1	416.7
	Staphylococcus epidermidis	9	?	3.1	?
Fungi	*Aspergillus niger*	181	23000	62.8	7986.1
	Candida albicans	2	327	0.7	113.5
	Saccharomyces cerevisiae	58	66	20.1	22.9

Table 2 – Whole-room disinfection (90 percent) with white and blue light. Source: Rutula et al. 2018.
* – Based on 0.5 mW/cm² irradiance.

As shown in Table 2, the optical power required to inactivate some pathogens can be ludicrous. Assuming a radiant efficiency of 70 percent, it would require an electrical load of 900 watts to over 100 kilowatts to control an *ASPERGILLUS NIGER* colony in a small room!

To be fair, some of these maximum doses are related to specific laboratory conditions that may not reflect those of whole-room applications. Nevertheless, the message is clear: the marketing efforts of both large and small luminaire manufacturers must sometimes be viewed with a critical eye.

CONCLUSIONS

As professional lighting designers, we would obviously prefer recommendations such as, “the visible light irradiance on the work plane shall be between 0.1 and 0.5 J/cm², and the daily radiant dose shall be no less than 12 hours.” Unfortunately, the reality is that we live in a dirty world with innumerable species and strains of pathogens that visible light cannot inactivate by even 90 percent without impractical irradiance levels and radiant doses.

The studies cited in this review have demonstrated that visible light has antimicrobial properties under carefully controlled laboratory conditions and (to a lesser extent) in hospital settings that were already designed to minimize the prevalence of pathogens through HEP-filtered air and daily terminal

cleaning. They also however clearly demonstrate that their results cannot be extrapolated to predict the performance of visible light disinfection systems in generic whole rooms, let alone provide evidence and support for lighting design guidelines.

In summary, visible light disinfection technology may be useful in some applications, but it is by no means a panacea. When designing or specifying a disinfection system, both the lighting designer and the client will need to thoroughly understand the capabilities and limitations of the technology, and agree upon its purpose.

As for validation of the installed system … that is another topic entirely.

ACKNOWLEDGEMENTS

Thanks to Doug Steel of NeuroSense, Martin Hessling of the Institute of Medical Engineering and Mechatronics, Ulm University of Applied Sciences, and David Woodward of Signify for their thoughtful and detailed review comments.

REFERENCES

Aldahan. A. S., et al. 2016. "Sun Exposure in History," JAMA Dermatology 152(8):896. https://doi.org/10.1001/jamadermatol.2015.5660.

Amin, R. M., et al. 2016. "Antimicrobial Blue Light Inactivation of *PSEUDOMONAS AERUGINOSA* by Photo-Excitation of Endogenous Porphyrins: In Vitro and In Vivo Studies," Lasers in Surgery and Medicine 48(5):562-568. https://doi.org/10.1002/lsm.ss474.

ASTM. 2020. G173-03(2020), Standard Tables for Reference Solar Spectral Irradiances: Direct Normal and Hemispherical on 37° Tilted Surface. ASTM International.

Bache, S. E., et al. 2012. "Clinical Studies of the High-Intensity Narrow-Spectrum Light Environmental Decontamination System (HINS-light EDS) for Continuous Disinfection in the Burn Unit Inpatient and Outpatient Settings," Burns 38:68-79. https://doi.org/10.1016/j.burns.2011.03.008.

Bache, S. E., et al. 2017. "Universal Decontamination of Hospital Surfaces in an Occupied Inpatient Room with a Continuous 405 nm Light Source," J. Hospital Infection 98(1):P67-73. https://doi.org/10.1016/j.jhin.2017.07.010.

Bumah, V. V., et al. 2013. "Wavelength and Bacterial Density Influence the Bactericidal Effect of Blue Light on Methicillin-Resistant *STAPHYLOCOCCUS AUREUS* (MSRA)," Photomedicine and Laser Surgery 31(3):547-553. https://doi.org/10.1089/pho.2012.3461.

Bumah, V. V., et al. 2013. "Wavelength and Bacterial Density Influence the Bactericidal Effect of Blue Light on Methicillin-Resistant *STAPHYLOCOCCUS AUREUS* (MSRA)," Photomedicine and Laser Surgery 31(3):547-553.

Bumah, V. S., et al. 2020. "Pulsed 450 nm Blue Light Suppresses MRSA and *PROPIONIBACTERIUM ACNES* in Planktonic Cultures and Bacterial Biofilms," J. Photochemistry & Photobiology B: Biology 202:111702. https://doi.org/10.1016/j.jphotobiol.2019.111702.

Christensen, T., et al. 2021. "Violet-Blue Light Exposure of the Skin: Is There Need for Protection?", Photochemical & Photobiological Sciences 20:615-625. https://doi.org/10.1007/s43630-021-00043-9.

Dai, T., et al. 2012. "Blue Light for Infectious Diseases: *PROPIONIBACTERIUM ACNES*, *HELICOBACTER PYLORI*, and Beyond?", Drug Resistance Update 15(4):223-236. https://doi.org/10.1016/j.drup.2012.07.001.

De Santis, R., et al. 2020. "Rapid Inactivation of SARS-CoV-2 with LED Irradiation of Visible Spectrum Wavelengths," J. Photochemistry and Photobiology. https://doi.org/10.1016/j.jpap.2021.100082.

Dougall, L. R., et al. 2018. "Efficacy of Antimicrobial 405 nm Blue-Light for Inactivation of Airborne Bacteria," Proc. SPIE 10479, 107491G. https://doi.org/10.1117/12.2289987.

Downes, A., and T. Blunt. 1877. "Research on the Effect of Light Upon Bacteria and Other Organisms," Proc. Royal Society of London 26:488-500.

Enwemeka, C. S., et al. 2008. "Visible 405 nm SLD Light Photo-Destroys Methicillin-Resistant *STAPHYLOCOCCUS AUREUS* (MRSA) *IN VITRO*," Lasers in Surgery and Medicine 40(10):734-737. https://doi.org/10.1002/lsm.20724.

Enwemeka, C. S., et al. 2020. "Light as a Potential Treatment for Pandemic Coronavirus Infections: A Perspective," J. Photochemistry & Photobiology B: Biology 207:111891. https://doi.org/10.1016/j.jphotobiol.2020.111891.

Enwemeka, C. S., et al. 2021a. "The Role of UV and Blue Light in Photo-eradication of Microorganisms," J. Photochemistry & Photobiology 8:100064. https://doi.org/10.1016/j.jpap.2021.100064.

Enwemeka, C. S. et al. 2021a. "Pulsed Blue Light Inactivates Two Strains of Human Coronavirus," J. Photochemistry and Photobiology B: Biology 222:112282. https://doi.org/j.photobiol.2021.112282.

Freeman, S., et al. 2022. “Systematic Evaluating and Modeling of SARS-CoV-2 UVC Disinfection,” Scientific Reports (2022)12:5869. https://doi.org/10.1038/s41598-022-09930-2.

Gillespie, J. B., et al. 2017. “Efficacy of Pulsed 405-nm Light-Emitting Diodes for Antimicrobial Photodynamic Inactivation: Effects of Intensity, Frequency, and Duty Cycle,” Photomedicine and Laser Surgery 35(3):150-156. https://doi.org/pho.2016.4179.

Grzybowski, A., and K. Pietrzak. 2012. “From Patient to Discoverer – Niels Ryberg Finsen (1860 – 1904) – the Founder of Phototherapy in Dermatology,” Clinics in Dermatology 30:451-455. https://doi.org/10.1016/j.clindermatol.2011.11.019.

Guffey, J. S., and J. Wilborn. 2007. “*IN VITRO* Bactericidal Effects of 405-nm and 470-nm Blue Light,” Photomedicine and Laser Surgery 24(6):684-688. https://doi.org/10.1089/pho.2006.24.684.

Guffey, J. S., et a. 2013. “Evidence of Resistance Development by *STAPHYLOCOCCUS AUREUS* to an *IN VITRO*, Multiple Stage Application of 405 nm Light for a Supraluminous Diode Array,” Photomedicine and Laser Surgery 31(4):179-182. https://doi.org/10.1089/pho.2012.3450.

Gwynne, P. J., and M. P. Gallagher. 2018. “Light as a Broad-Spectrum Antimicrobial,” Frontiers in Microbiology 9 Article 119. https://doi.org/10.3389/fmicb.2018.00119.

Halstead, F. D., et al. 2019. “Violet-Blue Light Arrays at 405 nm Exert Enhanced Antimicrobial Activity for Disinfection of Monomicrobial Nosocomial Biofilms,” Applied and Environmental Microbiology 85(21): 1-16. https://doi.org/10.1128/AEM.01346-19.

Hamblin, M. R., and T. Hasan. 2004. “Photodynamic Therapy: A New Antimicrobial Approach to Infectious Disease?”, Photochemistry & Photobiology Sciences 3(5):436-450. https://doi.org/10.1039/b311900a.

Hessling, M., et al. 2017. “Photoinactivation of Bacteria by Endogenous Photosensitizers and Exposure to Visible Light of Different Wavelengths – A Review on Existing Data,” FEMS Microbiology Letters 367. https://doi.org/10.1093/femsle/fnw270.

Hessling, M., et al. 2022a. “Review of Virus Inactivation by Visible Light,” Photonics 9:113. https://doi.org/10.3390/photonics9020113.

Hessling, M., et al. 2022b. “Surface Disinfection with White-Violet Illumination Device,” AIMS Bioengineering 9)2):93-101. https://doi.org/10.3934/bioeng.2022008.

Hönes, K., et al. 2018. “405 nm and 450 nm Photoinactivation of *SACCHAROMYCES CEREVISIAE*,” European Journal of Microbiology and Immunology 8(4):142-148. https://doi.org/10.1556/1886.2018.00023.

Huang, Y., et al. 2020. “Inactivation Efficacy of 405 nm LED Against *CRONOBACTER SAKAZAKII* Biofilm,” Frontiers in Microbiology 11:610077. https://doi.org/10.3389/fmicb.2020.610077.

ICNIRP. 2013. “ICNIRP Guidelines on Limits of Exposure to Incoherent Visible and Infrared Radiation.” Health Physics 105(10:74-96. https://www.icnirp.org/cms/upload/publications/ICNIRPVisible_Infrared2013.pdf

Kowalski, W. 2009. Ultraviolet Germicidal Irradiation Handbook: UVGI for Air and Surface Disinfection. New York, NY:Springer.

Kumar, A., et al. 2015. “Kinetics of Bacterial Inactivation by 405 nm and 520 nm Light Emitting Diodes and the Role of Endogenous Coproporphyrin on Bacterial Susceptibility,” J. Photochemistry and Photobiology 149:37-44. https://doi.org/10.1016/j.jphotobiol.2015.05.005.

Lau, B., et al. 2021. “High Intensity Violet Light (405 nm) Inactivates Coronaviruses in Phosphate Buffered Saline (PBS) and on Surfaces”, Photonics 101(8):414. https://doi.org/10.3390/photonics8100414.

Leanse, L. G., et al. 2018. “Evaluating the Potential for Resistance Development to Antimicrobial Blue Light (at 405 nm) in Gram-Negative Bacteria: *IN VITRO* and *IN VIVO* Studies,” Frontiers in Microbiology 2018.024043. https://doi.org/10.3389/fmicb.2018.02403.

Lipovsky, A., et al. 2009. “Sensitivity of *STAPHYLOCOCCUS AUREUS* Strains to Broadband Visible Light,” Photochemistry and Photobiology 85:255-260. https://doi.org/10.1111/j.1751-1097.2008.00429.x.

Maclean, M., et al. 2008. “High-Intensity Narrow-Spectrum Light Inactivation and Wavelength Sensitivity of *STAPHYLOCOCCUS AUREUS*,” FEMS Microbiology Letters 285:227-232. https://doi.org/10.1111/j.1574-6968.2008.01233.x.

Maclean, M., et al. 2010. “Environmental Decontamination of a Hospital Isolation Room Using High-Intensity Narrow-Spectrum Light,” J. Hospital Infection 76:247-251. https://doi.org/10.1016/j.jhin.2010.07.010.

Maclean, M., et al. 2013. “Continuous Decontamination of an Intensive Care Isolation Room During Patient Occupancy Using 405 nm Light Technology,” J. Infection Prevention 14(5):176-181. https://doi.org/10.1177/1757177413483646.

Maclean, M., et al. 2014. “405 nm Light Technology for the Inactivation of Pathogens and its Potential Role for Environmental Disinfection and Infection Control,” J. Hospital Infection 88(1):1-11. https://doi.org/10.1016/j.hnin.2014.06.004.

McKenzie, K., et al. 2013. “Photoinactivation of Bacteria Attached to Glass and Acrylic Surfaces by 405 nm Light: Potential Application for Biofilm Decontamination,” Photochemistry and Photobiology 8(9):927-935. https://doi.org/10.1111/php.12077.

Møller, K. I., et al. 2005. “How Finsen’s Light Cured Lupus vulgaris,” Photodermatology, Photoimmunology & Photomedicine 21(3):118-124. https://doi.org/10.1111/j.1600-0781.2005.00159x.

Murdoch, L. E., et al. 2013. “Lethal Effects of High Intensity Violet 405-nm Light on *SACCHAROMYCES CEREVISIAE*, *CANDIDA ALBICANS* and on Dormant and Germinating Spores of *ASPERGILLUS NIGER*,” Fungal Biology 117(7-8):519-527. https://doi.org/10.1016/j.funbio.2013.05.004.

Murrell, L. J., et al. 2019. “Influence of a Visible-Light Continuous Environmental Disinfection System on Microbial Contamination and Surgical Site Infections in an Orthopedic Operating Room,” American J. Infection Control 47:804-810. https://doi.org/10.1016/j.ajic.2018.12.002.

Plavskii, V. Y., et al. 2018. “Porphyrins and Flavins as Endogenous Acceptors of Optical Radiation of Blue Spectral Region Determining Photoinactivation of Microbial Cells,” J. Photochemistry and Photobiology 183:172-183. https://doi.org/10.1016/j.photobiol.2018.04.021.

Ramakrishnan, P., et al. 2009. “Cytotoxic Reponses to 405-nm Light Exposure in Mammalian and Bacterial Cells: Involvement of Reactive Oxygen Species,” Toxicology In Vitro 23:54-62. https://doi.org/10.1016/j.tiv.2016.02.011.

Rathnasinghe, R., et al. 2021. “The Virucidal Effects of 405 nm Visible Light on SARS-CoV-2 and Influenza A Virus,” Scientific Reports 11(11):19470. https://doi.org/10.1038/s41598-021-97797-0.

Rutala, W. A., et al. 2018. “Antimicrobial Activity of a Continuous Visible Light Disinfection System” Infectious Control Hospital Epidemiology 39(10):1250-1258. https://doi.org/20.1.17/ice.2018.200.

Schuit, M., et al. 2020. “The Influence of Simulated Sunlight on the Inactivation of Influenza Virus in Aerosols,” J. Infectious Diseases 2020:221:372-378. https://doi.org/10.1093/infdis/jiz582.

Stasko, N., et al. 2021. “Visible Blue Light Inhibits Infection and Replication of SARS-CoV-2 at Doses that are Well-Tolerated by Human Respiratory Tissue,” Scientific Reports 11:20595. https://doi.org/10.1038/s41598-021-99917-2.

Tomb, R. M., et al. 2014. “Inactivation of *STREPTOMYCES* phage F C31 by 405 nm Light: Requirements for Exogenous Photosensitizers?”, Bacteriophage 1:1-6. https://doi.org/10.4161/bact.32129.

Tomb, R. M., et al. 2017a. “Assessment of the Potential for Resistance to Antimicrobial Violet-Blue Light in Staphylococcus aureus,” Antimicrobial Resistance and Infection Control 6 Article 100. https://doi.org/10.1186/s13756-017-0261-5.

Tomb, R. M., et al. 2017b. “New Proof-of-Concept in Viral Inactivation: Virucidal Efficacy of 405 nm Light Against Feline Calicivirus as a Model for Norovirus Decontamination,” Food Environmental Virology 9:159-167. https://doi.org/10.1007/s12560-016-9275-z.

Tomb, R. M., et al. 2018. “Review of the Comparative Susceptibility of Microbial Species to Photoinactivation Using 380-480 nm Violet-Blue Light, Photochemistry and Photobiology 94(3):445-458. https://doi.org/10.1111/php.12833.

Ward, H. M. 1894. “The Action of Light on Bacteria – III,” Philosophical Trans. Royal Society of London B: Biology 185:961-986.

Light Pollution Information

QUANTIFYING LIGHT POLLUTION SOURCES

Ian Ashdown, P. Eng., FIES, Senior Scientist, SunTracker Technologies Ltd. Published: 22/02/28

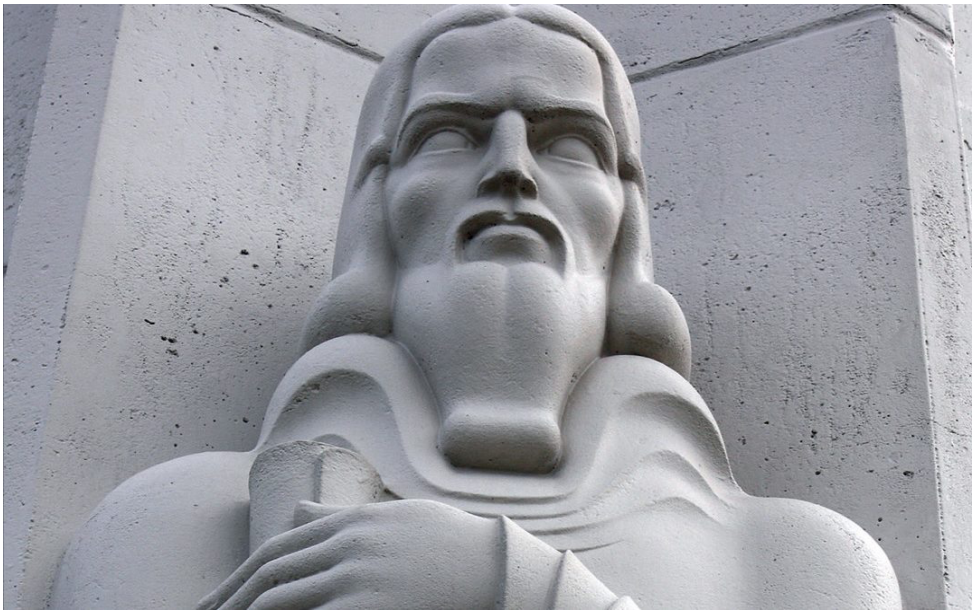

THE QUINTIC ROOT OF HIPPARCHUS

UPDATED 22/02/28

Nighttime light pollution is sadly familiar to all of us. While our grandparents and great-grandparents may talk fondly of seeing the Milky Way in their youth, with thousands of stars scattered across the dark summer sky, we are mostly content with seeing a few dozen stars through the never-ending dusk of urban and suburban skies.

As professional lighting designers, we know the solutions. First, we need to limit the amount of light that is uselessly directed or reflected upwards into the night sky from streetlights and outdoor area lighting. Second, we need to minimize the relative amount of blue light generated by the light sources. Third, we should dim or turn off the lighting when it is not needed. Three simple but effective solutions.

The question is, how do we quantify these solutions? What does it mean, for example, to “minimize the relative amount of blue light”? Indeed, how do we even define “blue light?” More important, what is the result of doing so? Given two light sources – for example, 2700K and 3000K LED streetlights – which is the better choice in terms of reducing nighttime skyglow? Is it even worth worrying about the difference?

What we are really asking here is, what is the relationship between the spectral power distribution (SPD) of a light source and its contribution to nighttime sky glow? If we know the answer to this

question, we can make quantitative and hence informed judgements when choosing exterior luminaires for street and area lighting.
What we need is (yet another) lighting design metric.

CORRELATED COLOR TEMPERATURE

At present, we are advised to simply choose luminaires with low CCTs. Indeed, the International Dark-Sky Association mandates luminaires with CCTs of 3000K or lower for its IDA Fixture Seal of Approval program, and is recommending luminaires with CCTs of no more than 2200K. Unpublished studies of over one thousand commercial LEDs have shown a strong correlation between CCT and the relative amount of blue light, so this is arguably a reasonable approach.

The problem however is that the 3000K limit is entirely prescriptive. If there is an application where a higher CCT is desired or even necessary, there is no opportunity for lighting designers to make a design decision based on factual information.

OTHER METRICS

Several other design metrics have been proposed, all with various shortcomings. For example, the scotopic-photopic ratio (S/P) may provide a reasonable indication of the relative amount of blue light in an SPD, but it is based solely on the human visual system. It may be useful for ranking light sources according to their relative blue light content, but it is not a quantitative measure.

Another approach is to specify an arbitrary division between blue and “not blue” light (typically 500 nm or 520 nm) and calculate the relative blue light content directly from the SPD. This approach is based solely on the SPD, with no reference to the human visual system or the illuminated environment. As such, it yields a metric that is useful only for ranking light sources according to their relative blue light content; it is not a quantitative measure.

What is needed is a metric that takes into account:

- Spectral power distribution;
- Photopic vision;
- Scotopic vision; and
- Atmospheric scattering

as these are the components of what we perceive as artificial sky glow and hence light pollution.

ANCIENT HISTORY

To develop a quantitative light pollution metric, we need to start at the desired end result and work backwards. To do so, we need to go back over two millennia to the time of Hipparchus of Nicaea (190 – c. 120 BC). Hipparchus was a Greek astronomer, geographer, and mathematician. Considered possibly the greatest astronomer of antiquity, he compiled the first comprehensive star catalog in the Western world. While this catalog has been lost to the mists of time, it likely contained at least 850 stars. More important for our needs, he is conjectured to have ranked the apparent magnitude (visual brightness) of stars on a scale of 1 (brightest) to 6 (faintest).

Moving forward in time some two thousand years, an English astronomer named Norman Robert Pogson was working at the Madras observatory in India when in 1856, he decided to place Hipparchus's apparent magnitude scale on a firm mathematical footing.

Figure 1 – N. R. Pogson.

Noting that the perceived brightness of a point source of light varies approximately logarithmically with intensity, and that the photometric intensity of a first-magnitude star was approximately one hundred times that of a sixth-magnitude star, he proposed that a difference of one magnitude be equal to $100^{1/5}$, or about 2.512 (Pogson's Ratio), in intensity (FIG. 2). Hence the fifth, or "quintic," root of Hipparchus.

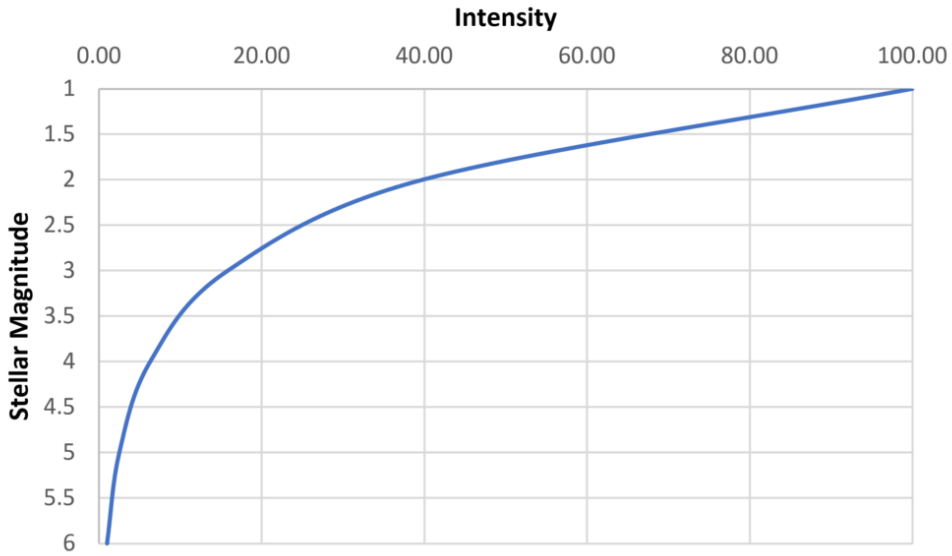

Figure 2 – Apparent magnitude versus intensity.

Hipparchus' apparent magnitude scale is open-ended – the magnitude of the brightest star Sirius is -1.46 (note the negative value), while large amateur telescopes are capable of detecting stars as faint as 16 on exceptionally clear nights. The number of visible stars with a given magnitude or brighter varies with latitude and season, but Table 1 provides a reasonable average estimate.

Apparent Magnitude	Number of Stars
1	15
2	48
3	171
4	513
5	1602
6	4800

Table 1 – Typical number of visible stars.

The point here is not the exact number of stars that are visible, but that the number depends on the sky brightness(or more properly, sky *LUMINANCE*). The faintest stars that can be seen on an exceptionally clear and dark night with fully dark-adapted eyes (i.e., scotopic vision) is about magnitude 6. In an area with a lot of light pollution, the limiting magnitude due to artificial sky glow can be as low as 2 or 3.

This is something that elementary school children can explain to their great-grandparents: the more light pollution there is, the fewer stars that can be seen. If we can calculate the difference in limiting magnitude due to light sources with different SPDs, all other factors being equal, we will have a quantitative light pollution metric.

TYPICAL OUTDOOR LIGHT SOURCES

Spectral power distributions for both luminaires and light sources (lamps and LED modules) are almost impossible to obtain from their manufacturers. Fortunately, CIE 015:2018, Colorimetry, Fourth Edition (CIE 2018) publishes the SPDs of two typical high-pressure sodium lamps, three metal halide lamps, and four light-emitting diodes that are representative of the light sources typically used for outdoor lighting applications.

Table 2 enumerates these light sources, along with the SPDs of anonymous products representing 2200K white light, phosphor-coated amber, and narrowband (quasimonochromatic) amber LEDs that are recommended by the International Dark-Sky Association.

Light Source	Description
CIE HP1	1950K HPS
CIE HP2	2500K HPS
CIE HP3	3100K MH
CIE HP4	4000K MH
CIE HP5	4000K MH
CIE B1	2700K LED
CIE B2	3000K LED
CIE B3	4000K LED
CIE B4	5000K LED
Generic 2200K	2200K LED
Generic PC Amber	PC amber LED
Generic Amber	Narrowband amber LED

Table 2 – Typical outdoor light sources.

To simplify matters, we can assume that two or more different light sources have the same luminous intensity distribution and luminous flux output; the only difference is their spectral power distribution. Given this, we begin by choosing two light sources, say CIE HP1 and CIE B1, for comparison, with their normalized SPDs as shown in Figure 3. The physical sources they represent – a high-pressure sodium lamp and a single LED – will obviously have different luminous flux outputs. We therefore need to scale these SPDs such that they represent the same luminous flux.

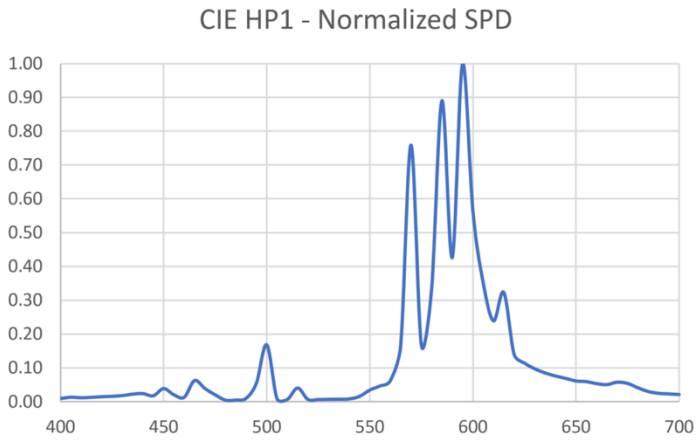

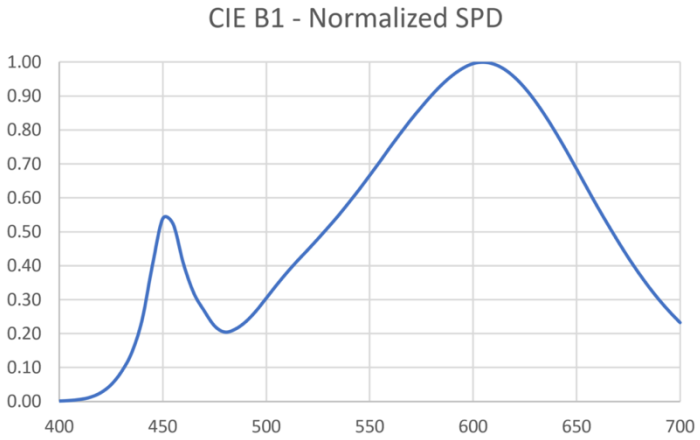

Figure 3 – Normalized SPDs

PHOTOPIC VISION

Lighting design for roadway and area lighting applications is typically based on photopic illuminance values. If we multiply each tabulated value of the light sources SPDs on a per-wavelength basis by the corresponding value of the photopic efficiency function V(λ) of Figure 4, we can sum the resultant values and multiply this sum by a constant to obtain the lumens emitted by the light source.

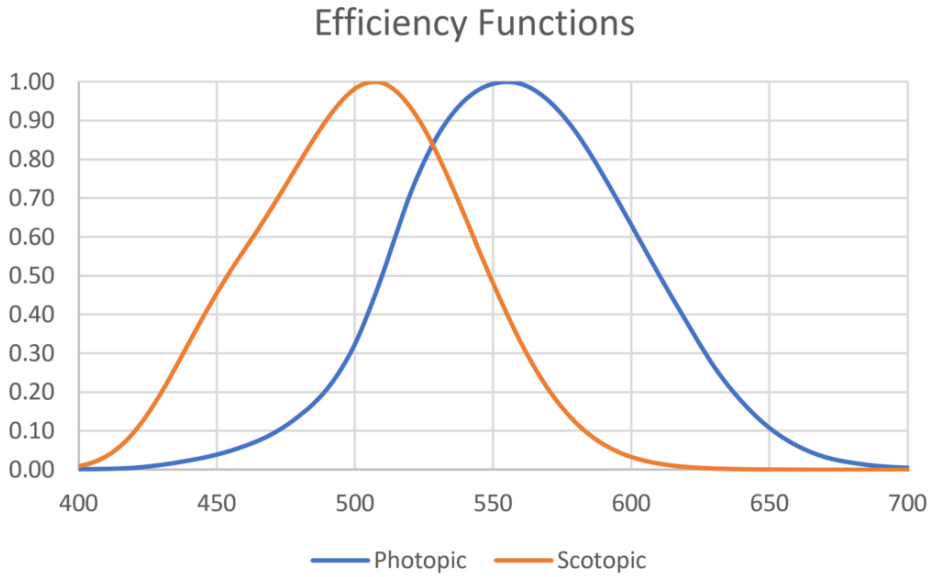

Figure 4 – Visual efficiency functions.

The constant is not important here, as we only need to ensure both light sources are emitting the same number of lumens (i.e., luminous flux). In the example given here, the sum for the CIE HP1 lamp is 4.373, while the sum for the CIE B1 source is 14.969. If we nominate CIE HP1 as our baseline light source, we then need to scale the CIE B1 SPD by 4.373 / 14.969 = 0.292. The scaled SPDs are shown in Figure 5.

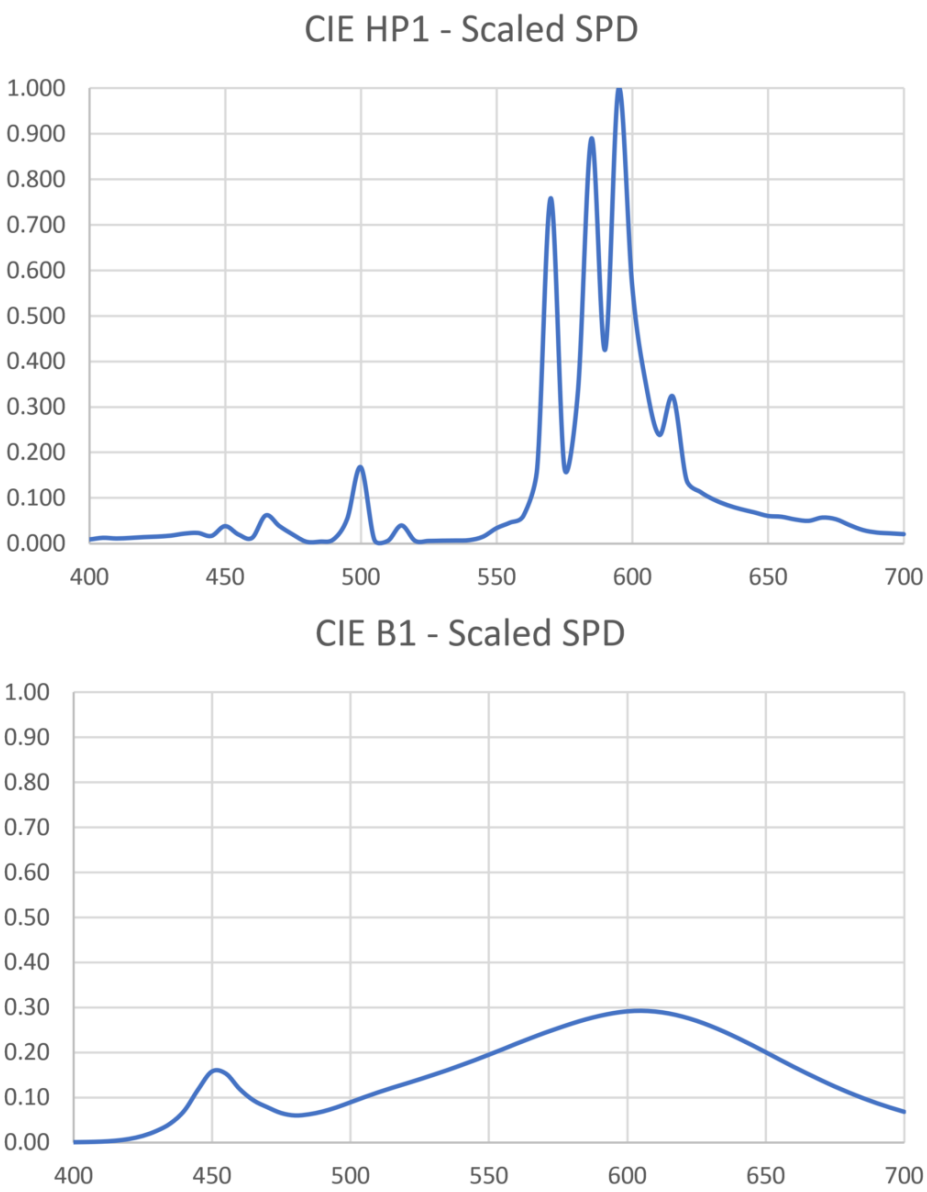

Figure 5 – Scaled SPDs.

ATMOSPHERIC SCATTERING

Our atmosphere preferentially scatters blue light, which is why the sky is blue on a clear day. This is caused by Rayleigh scattering from nitrogen and oxygen molecules, but there is also Mie scattering, which is caused by aerosols such as water droplets, dust and smog. Mie scattering is wavelength-independent, which is why fog and clouds, for example, are gray.

At a distance of 80 kilometers (50 miles) from a city center, both Rayleigh and Mie scattering contribute to sky glow that is caused by electric lighting. A study by Aubé (2015) provides an approximate scattering function:

$S = (550/\lambda)^{2.7}$

where λ is the wavelength in nanometers. This function (which assumes that we are looking straight up at the zenith rather than towards the horizon) is plotted in Figure 6.

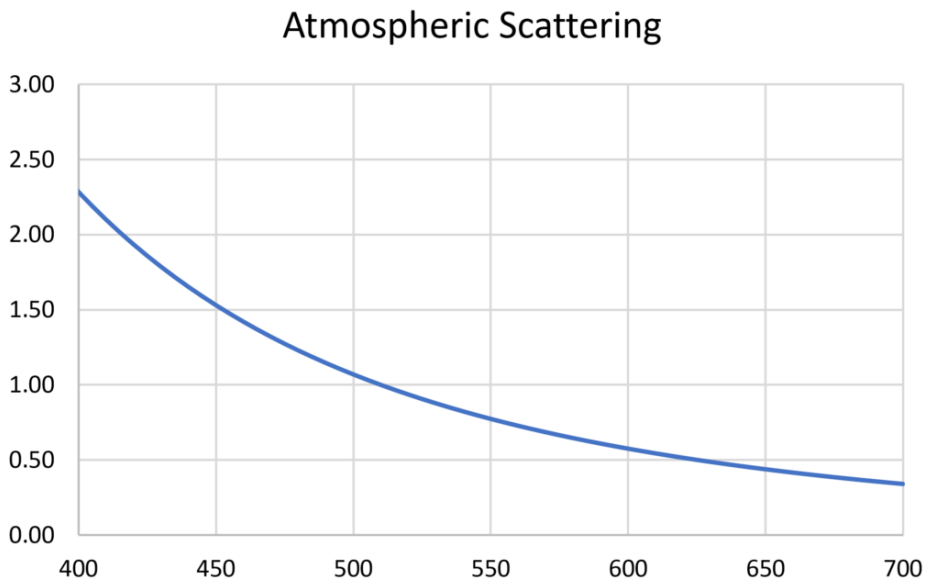

Figure 6 – Atmospheric scattering function.

If we multiply the scaled light source SPDs by the atmospheric scattering on a per-wavelength basis, we obtain the scattering SPDs shown in Figure 7. These represent the spectrum of the sky glow contributed by the light sources. (There is also natural sky glow caused by airglow, zodiacal light, and scattered starlight, with a typical limiting magnitude of 21.)

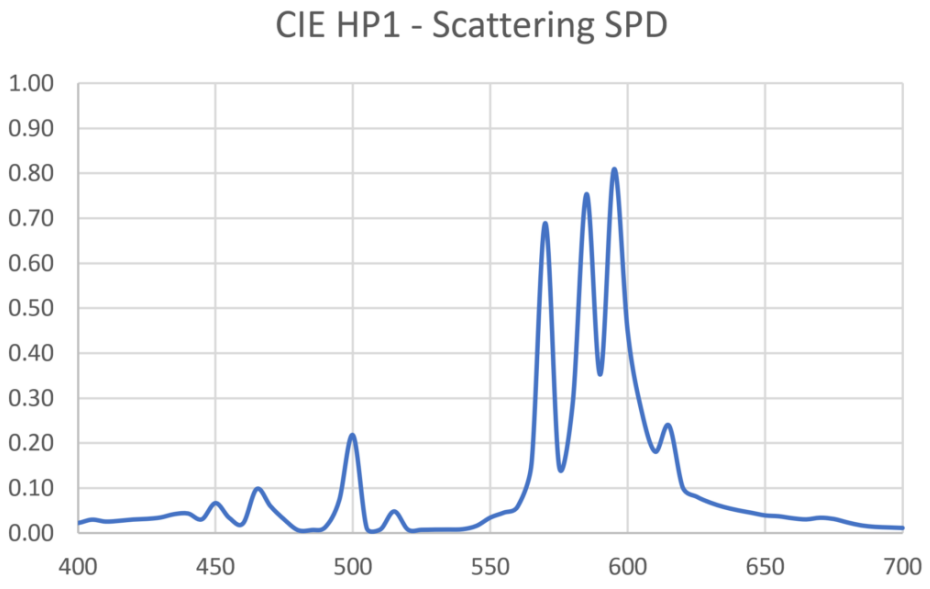

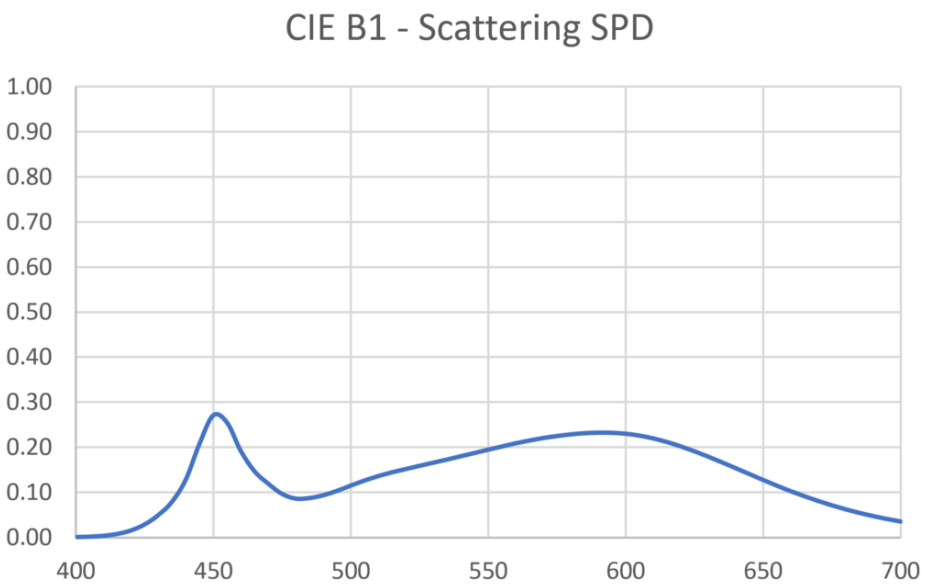

Figure 7 – Scattering SPDs.

SCOTOPIC VISION

Under dark skies with fully dark-adapted eyes, the spectral response of our eyes is described by the scotopic efficiency function V'(λ), shown in Figure 4. We must therefore multiply each tabulated wavelength value of the scattering SPDs by the corresponding wavelength value of the scotopic efficiency function to obtain the scotopic SPDs shown in Figure 8.

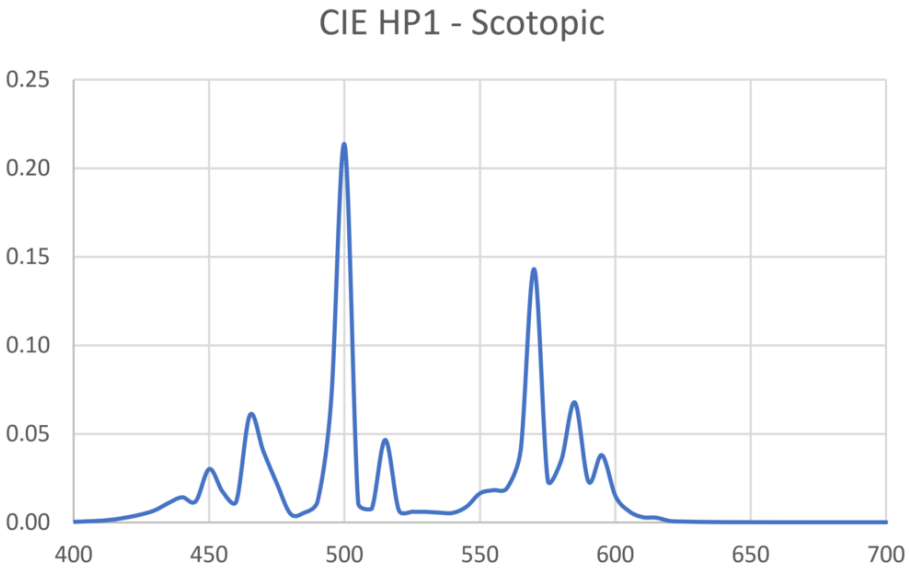

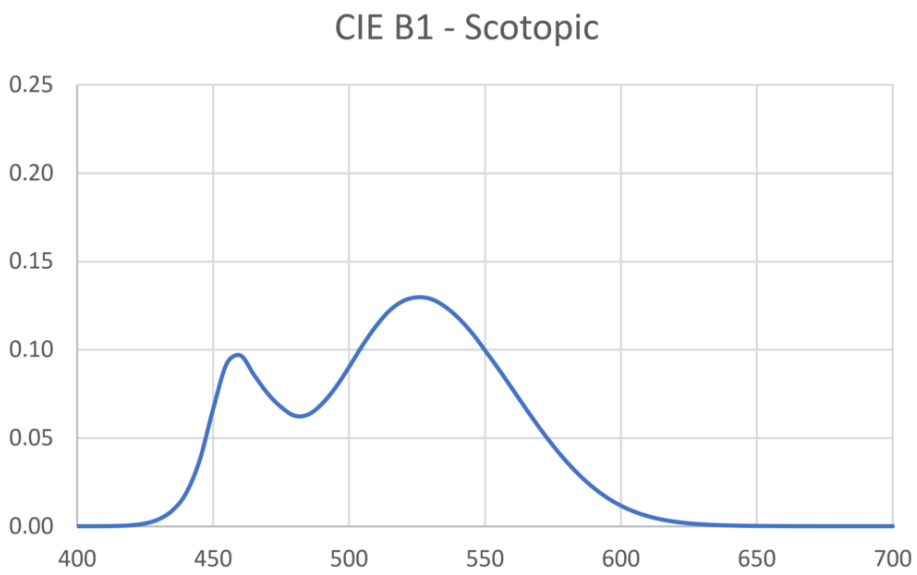

Figure 8 – Scotopic SPDs.

If we sum the tabulated wavelength values of each scotopic SPD and multiply by a constant, we could calculate the contribution to sky luminance. This however is not our goal – we simply want to know the relative contribution to sky luminance due to the SPD of each light source. For any given light source, we therefore divide the sum of the tabulated values of its scotopic SPD by the sum of the tabulated values of the scotopic SPD of our baseline light source CIE HP1. This gives us the relative scotopic luminance values enumerated in Table 3.

Light Source	Relative Scotopic Luminance
CIE HP1	1.00
CIE HP2	1.98
CIE HP3	2.64
CIE HP4	3.20
CIE HP5	3.64
CIE B1	2.34
CIE B2	2.60
CIE B3	3.50
CIE B4	3.82
Generic 2200K	1.53
Generic PC Amber	1.14
Generic Amber	0.32

Table 3 – Relative scotopic luminance.

RELATIVE LIMITING MAGNITUDE

Finally, we need to convert the relative scotopic luminance values to relative limiting magnitude values using Pogson's equation:

$$M_{limit} = -2.5 \log_{10}(L_{scotopic})$$

This equation accounts for our approximately logarithmic response to photometric intensity, and gives us the relative limiting magnitude values presented in Table 4.

Light Source	Relative Sky Luminance
CIE HP1 (baseline)	0.00
CIE HP2	-0.74
CIE HP3	-1.05
CIE HP4	-1.26
CIE HP5	-1.40
CIE B1	-0.92
CIE B2	-1.04
CIE B3	-1.36
CIE B4	-1.46
Generic 2200K	-0.46
Generic PC Amber	-0.14
Generic Amber	+1.23

Table 4 – Relative limiting magnitudes.

This then is the quantitative light pollution metric we have sought. The values are more usefully presented in Figure 9, where we can see at a glance how the different light sources compare.

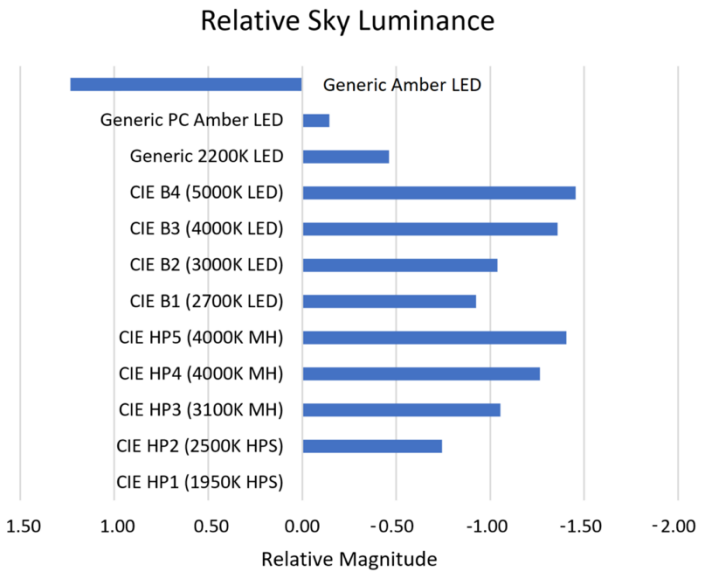

Figure 9 – Relative sky luminance.

It is further interesting to compare these results to that of percent blue content for each light source, as shown in Figure 10 (with a cut-off wavelength of 520 nm). The ranking is the same as the relative sky luminance shown in Figure 9, but the quantitative differences can be misleading.

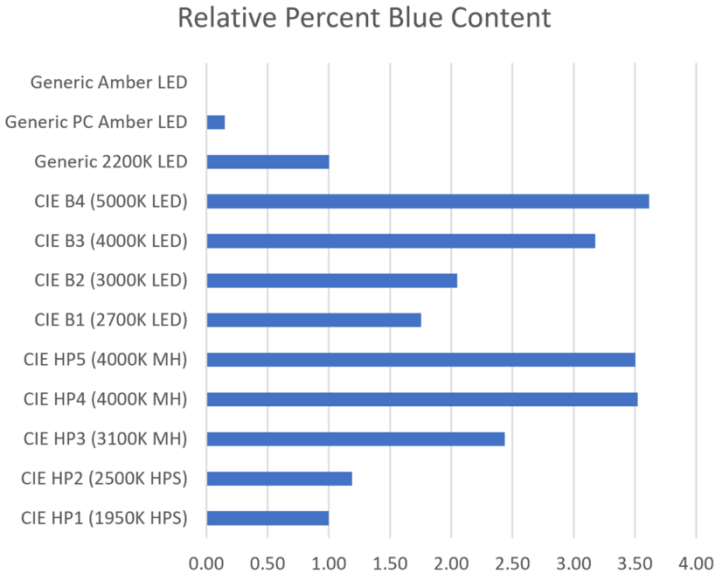

Figure 10 – Relative percent blue content.

METRIC CALCULATION

High-pressure sodium lamps from different manufacturers will likely have different SPDs, but the CIE HP1 lamp has the advantage of providing a standard baseline (i.e., a reference light source) for the proposed light pollution metric. With this, the calculation procedure for any target light source, present or future, consists of:

1. Normalize the reference and target SPDs.
2. Multiply SPDs by photopic efficiency function V(λ).
3. Sum tabulated values of resultant photopic SPDs.
4. Multiply photopic SPDs by sum divided by reference sum to produce scaled SPDs.
5. Multiply scaled SPDs by atmospheric scattering function.
6. Multiply scattering SPDs by scotopic efficiency function V'(λ).
7. Sum tabulated values of resultant scotopic SPDs.
8. Multiply scotopic SPDs by sum divided by reference sum.
9. Calculate relative limiting magnitude.

GREENHOUSE SUPPLEMENTAL LIGHTING

Horticultural light pollution is a particular concern, as the light levels needed for crops within greenhouses at night can be on the order of one hundred to one thousand times those required for roadway and area lighting.

The photosynthetic photon flux output of horticultural luminaires is measured in micromoles per second rather than lumens, and the spectral output is expressed as a spectral quantum distribution (SQD) rather than a spectral power distribution (SPD). However, these details become unimportant when relative values are considered.

The equation to convert an SPD to an SQD is:
$V_Q(\lambda) = V_P(\lambda) * \lambda * c$
where $V_P(\lambda)$ is the SPD value at wavelength λ, $V_Q(\lambda)$ is its corresponding SQD value, and c is a constant. The value of the constant is not important, as the SQD will be normalized afterwards.

High-pressure sodium lamps have been a mainstay of supplemental electric lighting for greenhouses since the 1960s, so we can again use the CIE HP1 lamp as a baseline reference source. The SPD and corresponding SQD for this lamp are shown in Figure 11. (The two distributions are almost identical, apart from the smaller peak at 500 nm; this is not necessarily true for all SPDs.)

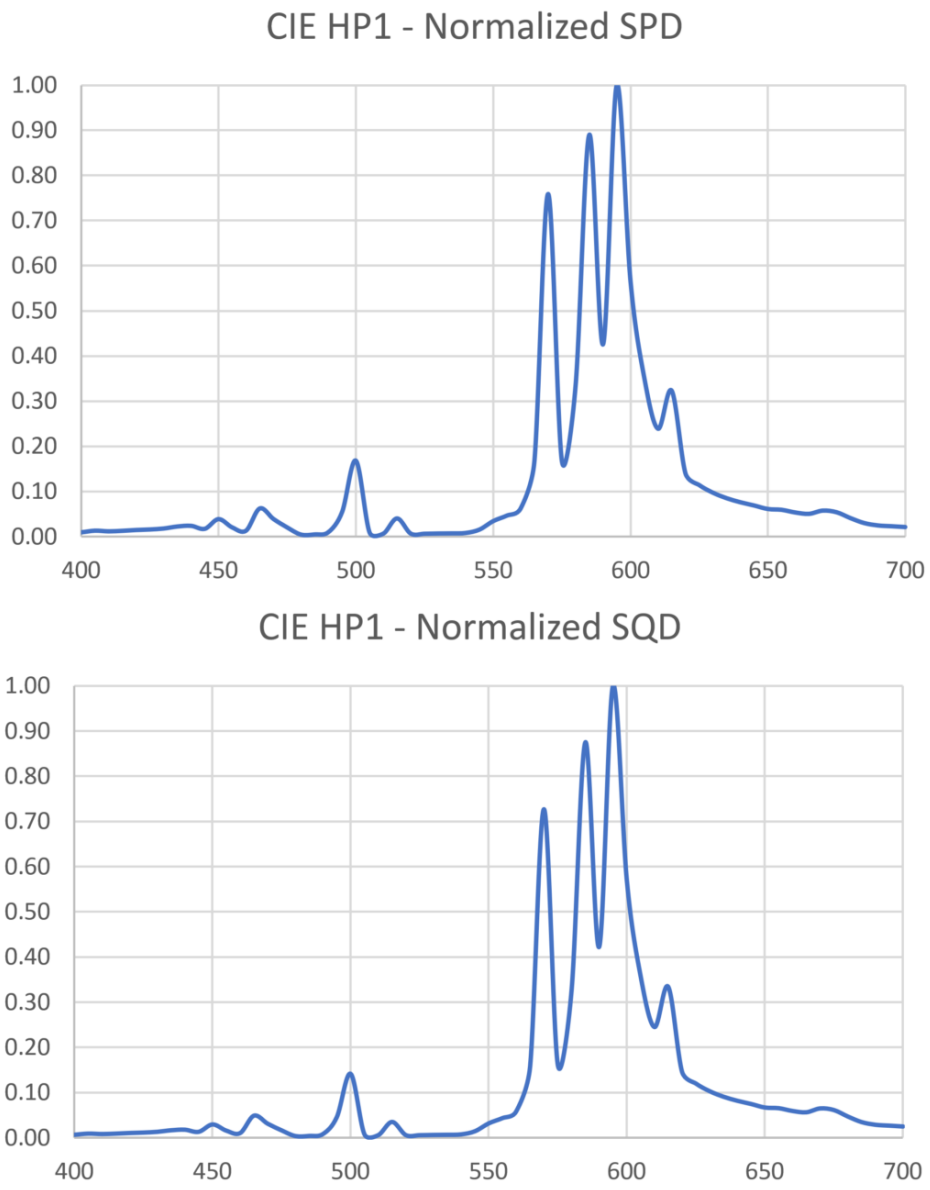

Figure 11 – Normalized SPD and SQD.

With this, we can consider two typical horticultural SQDs as shown in Figure 12. The luminaire labelled *HORT 1* has 450 nm blue and 660 nm red LEDS designed to maximize photosynthesis, while the luminaire labelled *HORT 2*includes phosphors that provide additional green light to benefit the plant growth and health.

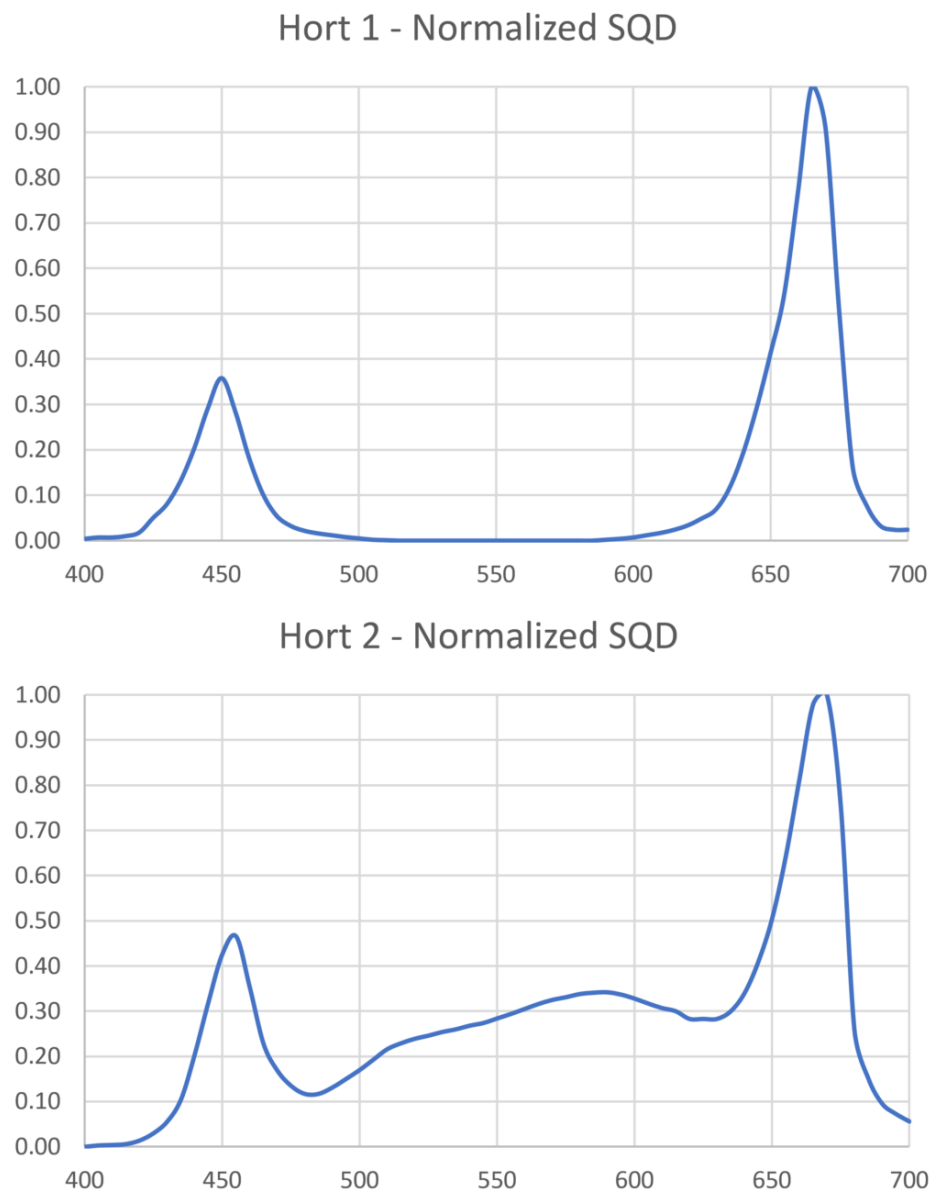

Figure 12 – Typical horticultural luminaire SQDs.

The calculation procedure for horticultural luminaires is somewhat different:

1. Convert reference SPD to normalized reference SQD.
2. Sum tabulated values of normalized SQDs.
3. Multiply normalized SQDs by sum divided by reference sum to produce target scaling factor.
4. Convert target SQD to normalized SPD.
5. Multiply target SPD by scaling factor.
6. Multiply SPDs by atmospheric scattering function.
7. Multiply scattering SPDs by scotopic efficiency function V'(λ).
8. Sum tabulated values of resultant scotopic SPDs.

9. Multiply scotopic SPDs by sum divided by reference sum.
10. Calculate relative limiting magnitude.
11.

Following this procedure, the relative limiting magnitude of the *HORT 1* luminaire is +0.16 (i.e., slightly better than the baseline HPS lamp), while the relative limiting magnitude of the *HORT 2* luminaire is -0.49 (i.e., about the same as a 2200K LED luminaire).

S/P RATIOS

About a decade ago, there was considerable academic interest in mesopic vision, where the perceived (not measured) luminance of objects depends on the scotopic-to-photopic (S/P) ratio of the light source and the photopic adaptation (i.e., background) luminance. This resulted in effective luminance multipliers being recommended by CIE 191:2010, Recommended System for Mesopic Photometry Based on Visual Performance (CIE 2010), and IES TM-12-12, Spectral Effects of Lighting on Visual Performance at Mesopic Lighting Levels (IES 2012).

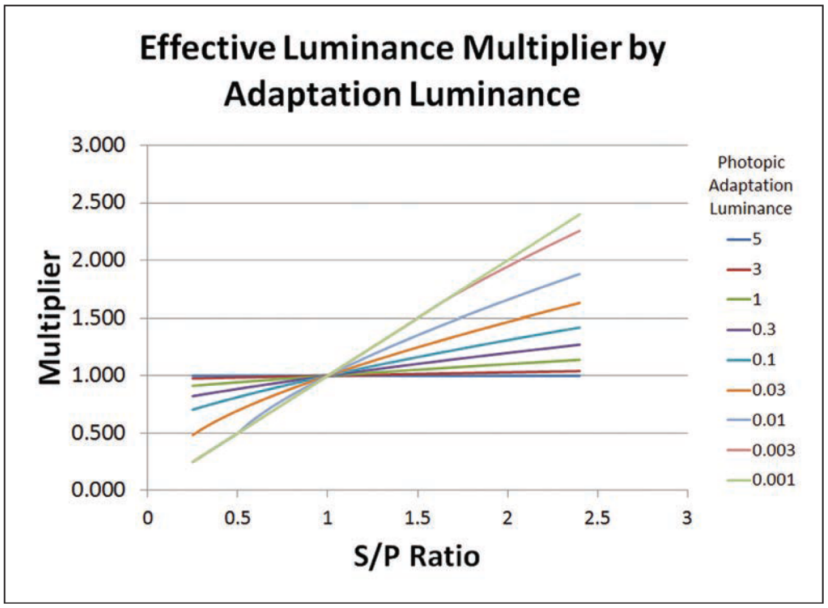

Figure 13 – Mesopic lighting multipliers. (Source: IES 2012.)

This concept was adopted by British Standard BS 5489-1, Code of Practice for the Design of Road Lighting, in 2013, but later mostly abandoned in the latest revision (BSI 2020). Today, it is recommended that the use of S/P ratios be discontinued when using white light sources with an CIE General Colour Rendering Index Ra greater than 70 (CIE 1995).

Light Source	S/P Ratio
CIE HP1 (baseline)	0.56
CIE HP2	1.06

CIE HP3	1.36
CIE HP4	1.59
CIE HP5	1.79
CIE B1	1.21
CIE B2	1.33
CIE B3	1.72
CIE B4	1.85
Generic 2200K	0.84
Generic PC Amber	0.71
Generic Amber	0.24

Table 5 – Light source S/P Ratios

One of the reasons for this recommendation is that S/P ratios favor light sources with higher CCTs (Table 5). By ignoring mesopic lighting multipliers for "white" light sources, the use of high-CCT LED light sources is discouraged.

This would appear to complicate matters if CIE HP1 is taken as the baseline light source – it has an S/P ratio of 0.56 and a CRI Ra value of 24. However, the minimum recommended illuminance for pedestrian walkways in rural areas is about two lux (e.g., IES 2014). If we assume a typical diffuse ground reflectance of 15 percent, this means that the adaptation luminance is about 0.3 cd/m^2.

Referring to Figure 13 (and also to Annex A of IES TM-12-12), the effective luminance multiplier for CIE HP1 is about 0.94. In other words, the effective luminance multiplier for white light sources compared to CIE HP1 is at most an insignificant six percent. (Calculation results within ten percent of the target illuminance are considered to meet the design goal.)

Narrow amber, PC amber, and 2200K LED light sources are not "white," as so the S/P ratios should, in accordance with BS 5489-1 recommendations, be applied. Again, however, we need to consider the minimum adaptation luminance of 0.3 cd/m^2. This is off the chart of Annex A, which covers the range of 0.001 to 0.1 cd/m^2. However, a reasonable extrapolation for the worst case of narrowband amber yields an effective luminance multiplier of 0.93.

Mesopic vision is also recognized by ANSI/IES RP-8-14, Roadway Lighting (IES 2014), which recommends that effective luminance multipliers "only be used to assess the luminances of off-road locations in applications for street lighting where the posted speed limit is 25 mph (40 km/h) or less" and "In cases where extraneous light sources or surroundings increase adaptation levels significantly above those of the pavement luminance, these factors are not appropriate."

For all practical purposes in outdoor nighttime lighting applications then, effective luminance multipliers based on the S/P ratio of the light source do not apply.

CONCLUSION

The primary advantages of the proposed metric are that:

1. It is based on a reasonable model of the physical and visual processes that result in our perception of light pollution;
2. It relies on a straightforward calculation procedure; and
3. The metric is simple enough for a schoolchild to explain.

To further explain the third point, the schoolchild does not need to explain how the metric is calculated. Rather, it becomes as simple as saying, “Bigger (negative) numbers means that we can see fewer stars in the night sky.” This is on par with saying, “Miles per gallon (MPG) is the distance that a car can travel on a gallon of fuel.” Explaining how this metric is calculated is an entirely different issue.

Some caution, however, should be taken in applying the metric to outdoor lighting design. For most applications, a difference of one-half magnitude is significant. Thus, there should be a good reason for specifying, for example, 4000K LED lighting rather than 3000K as recommended by the International Dark-Sky Association. (One argument might be that color discrimination is important.) The difference between the two may be only one-third magnitude, but it is still noticeable visually.

On the other hand, the difference between 2700K and 3000K LED lighting is only 0.08 magnitudes (based on the CIE SPDs). It would be difficult to argue that this is significant for any practical application if – a very big if – astronomical light pollution for visual star-gazing is the only design criterion. In general, lighting designers will need to take into consideration other factors, such as color discrimination for drivers and pedestrians, the effect of short-wavelength (“blue”) light at night on insects, birds, amphibians, fish, and mammals, color preferences of homeowners on residential and commercial streets, light-source temperature dependencies (especially narrowband amber LEDs), luminaire efficacy, capital and operating costs, and more.

While spectral power distribution data are rarely available from luminaire manufacturers in tabular form, this is not a particular problem. The light source SPDs published in CIE (2018) are more than adequate in calculating light pollution metrics for different classes of light sources. The point of this metric is not to provide immutable guidelines for lighting designers, but to provide quantifiable values on which to base these decisions.

ACKNOWLEDGEMENTS

The author thanks Eric Bretschneider and David Woodward for their useful and productive review comments.

REFERENCES

Aubé, M. 2015. “Physical Behaviour of Anthropogenic Light Propagation into the Nocturnal Environment,” Philosophical Transactions of the Royal Society B 370(1667):20140117.

BSI. 2020. BS 5489-1:2020, Code of Practice for the Design of Road Lighting, Part 1 – Lighting of Road and Public Amenity Areas. British Standards Institution.

CIE 1995. CIE 13.3-1995, Method for Measuring and Specifying Colour Rendering Properties of Light Sources. Vienna, Austria: CIE Central Bureau.

CIE. 2010. CIE 191:2010, Recommended System for Mesopic Photometry Based on Visual Performance. Vienna, Austria: CIE Central Bureau.

CIE. 2018. CIE 015:2018, Colorimetry, Fourth Edition. Vienna, Austria: CIE Central Bureau.

IES. 2012. IES TM-12-12, Spectral Effects of Lighting on Visual Performance at Mesopic Lighting Levels. New York, NY: Illuminating Engineering Society.

IES. 2014. ANSI/IES RP-8-14, Roadway Lighting. New York, NY: Illuminating Engineering Society.

ALL THINGS LIGHTING® ASSOCIATION

Suite 501 – 747 Fort Street
Victoria, BC Canada, V8W 3E9
www.allthingslighting.org

View this journal at https://www.allthingslighting.org/publications/